2020

Updating the Atmospheric and Health Effects Framework Model: Stratospheric Ozone Protection and Human Health Benefits

Stratospheric Protection Division
Office of Air and Radiation
U.S. Environmental Protection Agency
Washington, D.C. 20460

EPA Publication Number 430R20005
May 2020

Table of Contents

Executive Summary **1**

I. Introduction **2**

I.1 The AHEF Model 2

II. Updated Results **4**

II.1 Health Effects Results 4

II.1.1 Overview of Human Health Effects Estimated in the AHEF 4

II.1.2 Comparison with Historical Health Effects 6

II.1.3 Health Benefits of the Montreal Protocol 8

II.1.3.1 Health Effects for People Born in 1890–2100 9

II.1.3.2 Health Effects during the Period 1980–2100 9

II.1.3.3 Annual Incremental Incidence of Health Effects 10

II.2 EESC and Ozone Results 14

III. Model Overview and Updates **16**

III.1 Emissions Sub-Model 18

III.1.1 Sub-model Description 18

III.1.2 Updates 19

III.2 Ozone Depletion Sub-model 19

III.2.1 Sub-model Description 19

III.2.2 Updates 21

III.3 UV Radiation Sub-model 22

III.3.1 Sub-model Description 22

III.3.2 Updates 23

III.4 Exposure Sub-model 23

III.4.1 Sub-model Description 23

III.4.2 Updates 24

III.5 Health Effects Sub-model 24

III.5.1 Sub-model Description 24

III.5.2 Updates 26

IV. Potential Topics for Future Research **26**

IV.1 Other Geographies 27

IV.2 Fractional Chlorine Release 27

IV.3 Other Health Effect Relationships 27

IV.4 Non-compliance with Emissions Controls 28

References **29**

Appendix A. Glossary and Acronyms **33**

Appendix B. ODS Parameters **36**

Appendix C. Discussion of Assumptions at Simulation End **37**

Appendix D. Effects of Early-life Exposure Weighting **42**

Appendix E. Sensitivity of Effects Calculations to Assumptions About Race **43**

Appendix F. Estimation of Incremental Health Effects of Additional CFC-11 Emissions **47**

Preface

This report was prepared by the U.S. Environmental Protection Agency (EPA) with the support of its contractor, ICF. Key contributors included: Robert Landolfi, Cindy Newberg, Bella Maranion, and Elisa Rim from the EPA; Jessica Kyle, Mark Wagner, Helena Caswell, and Paula Garcia Holley from ICF; and Dr. Sasha Madronich and Dr. Julia Lee-Taylor from the National Center for Atmospheric Research (NCAR). This report describes updates to the EPA's Atmospheric and Health Effects Framework (AHEF), which models adverse human health effects associated with a depleted stratospheric ozone layer. The AHEF is updated regularly to reflect new information and science.

The initial report was drafted in 2019 and was peer reviewed by Dr. Nigel Paul of the Environment Centre at Lancaster University, Dr. Robyn Lucas of the National Centre for Epidemiology & Population Health at Australian National University, Dr. Stephen Montzka of the National Oceanic and Atmospheric Administration, and Dr. Tina Birmpili of the United Nations Environment Programme (UNEP) Ozone Secretariat. The peer reviewers were asked to draw upon their expertise in ozone depleting substance (ODS) emissions and ultraviolet (UV) radiation health modeling and science to comment on whether the data inputs, approach, and methodologies presented in the report reflect sound scientific and analytical practice, and adequately address the questions at hand. All comments of the peer reviewers were considered in finalizing this report.

Based on written comments received from the peer reviewers, the report includes a discussion of the sensitivity of human health effects calculations to assumptions about mapping race to skin type (in Appendix E) and a comparison of squamous cell carcinoma mortality from the University of Washington's Institute for Health Metrics and Evaluation (IHME, 2020) to the AHEF estimates. A scenario for the unexpected increased emissions of an ODS, CFC-11, was also developed by the Montreal Protocol's Science Assessment Panel, and results from a run in the AHEF are included in Appendix F. Comments received were also used to ensure the report text and references rely on the most recent information from the Montreal Protocol's Environmental Effects Assessment Panel (EEAP, 2019) and the American Cancer Society (ACS, 2020). A number of comments also identified areas for technical and expositional clarification and opportunities for future improvements.

The EPA wishes to acknowledge everyone involved in the development of this report and to thank the peer reviewers for their time, effort, and expert guidance. The involvement of the peer reviewers greatly enhanced the technical soundness of this report. The EPA accepts responsibility for all information presented and any errors contained in this document.

Executive Summary

Overexposure to ultraviolet (UV) radiation is a threat to human health. It can cause skin damage, eye damage, and suppress the immune system. Overexposure to UV radiation also interferes with environmental cycles, affecting organisms such as plants and phytoplankton that move nutrients and energy through the biosphere.

Human-made ozone-depleting substances (ODS) reduce the ozone concentration in the Earth's stratosphere. The stratospheric ozone layer acts as a protective shield from harmful UV radiation, so damage to it increases the amount of UV radiation reaching Earth's surface. More UV radiation means potentially more adverse human health effects, like skin cancer and cataract, as well as environmental damage. The 1987 *Montreal Protocol on Substances that Deplete the Ozone Layer* (Montreal Protocol) is an international treaty that protects and restores the ozone layer by phasing out the production and consumption of certain ODS.

The United States Environmental Protection Agency (EPA) uses its Atmospheric and Health Effects Framework (AHEF) model to assess the adverse human health effects associated with a depleted stratospheric ozone layer. The AHEF estimates the probable difference in skin cancer mortality, skin cancer incidence, and cataract incidence in the United States between different ODS emission scenarios.

This report describes a number of updates to the AHEF since its last update in 2015. These updates include changing various parameters to ensure the AHEF is based on up-to-date science, changes to methodologies to take advantage of newly available data, and modernization and streamlining of the underlying computer code to increase the usability and adaptability of the model.

This report explains in detail each of the updates made to the AHEF and provides an analysis of how these changes affect the health benefits estimated. With the current set of updates to the AHEF, the Montreal Protocol as amended and adjusted—compared with a scenario of no controls on ODS to reduce or avoid emissions—is now expected to prevent approximately 443 million cases of skin cancer, 2.3 million skin cancer deaths, and 63 million cataract cases for people in the United States born in the years 1890–2100.

The strengthening of the original Montreal Protocol with its subsequent amendments and adjustments accounts for a significant portion of these benefits, resulting in an estimated 230 million fewer skin cancers, 1.3 million fewer deaths, and 33 million fewer cataract cases than the original 1987 Montreal Protocol over the same period. The differences between these estimates and the estimates due to the Montreal Protocol as amended and adjusted in the previous paragraph are attributable to the original Montreal Protocol. This finding illustrates how reducing ODS emissions leads to increases in stratospheric ozone concentrations, thereby reducing overexposure to UV radiation and consequent adverse health impacts.

I. Introduction

Overexposure to ultraviolet (UV) radiation from the sun and man-made sources is a threat to human health. It can cause skin damage, eye damage, and suppress the immune system. Overexposure to UV radiation also interferes with environmental cycles, affecting organisms such as plants and phytoplankton, that move nutrients and energy through the biosphere. Earth's primary protection from solar UV radiation is the stratospheric ozone layer, which absorbs these high-energy UV rays before they reach Earth's surface.

In the 1970s, scientists discovered that the stratospheric ozone layer was thinning as a result of the use of chemicals that contained chlorine and bromine, which when broken down could destroy ozone molecules. The most common of these ozone-depleting substances (ODS) was a class of chemicals called chlorofluorocarbons (CFCs), which were widely used in a variety of industrial and household applications, such as aerosol sprays, plastic foams, and the refrigerant in refrigerators and in both car and building air-conditioning units. Scientific observations of the rapid thinning of the ozone layer over Antarctica from the late 1970s onward—often referred to as the "ozone hole"—supported international action to discontinue the use of CFCs.

In 1987, the United States joined 23 other countries and the European Union to sign the *Montreal Protocol on Substances that Deplete the Ozone Layer* (Montreal Protocol). This international treaty protects and restores the ozone layer by phasing out the production and consumption of certain ODS including CFCs, halons, methyl bromide, and hydrochlorofluorocarbons (HCFCs). Implementation of the Montreal Protocol has been successful at protecting the ozone layer and preventing the damage that could have occurred with continued and increasing ODS use. Since 1987, the Montreal Protocol has been amended and adjusted to expand the list of controlled substances and to adjust the phaseout of ODS production and consumption.[1]

I.1 The AHEF Model

In the 1980s, the United States Environmental Protection Agency (EPA) began assessing the health impacts on the U.S. population associated with ODS-induced changes in stratospheric ozone, both to better understand the adverse human health effects associated with a depleted stratospheric ozone layer and to quantify the benefits of policies that reduce ODS emissions and protect stratospheric ozone. These calculations informed the development of the EPA's Atmospheric and Health Effects Framework (AHEF) model in the 1990s. The EPA uses AHEF to estimate the probable changes in skin cancer mortality, skin cancer incidence, and cataract incidence in the United States that result from different ODS emission scenarios when compared to a baseline scenario. Changes in health effects are calculated either for (a) incremental changes associated with one policy scenario relative to another or (b) relative to a 1979–1980 baseline. The1979–1980 baseline refers to conditions pertaining to un-depleted

[1] For an overview of the amendments, please see U.S. EPA, 2019. For details on the amendments and adjustments, please see the section "The Evolution of the Montreal Protocol" in the 13th edition of the Montreal Protocol handbook: https://ozone.unep.org/treaties/montreal-protocol-substances-deplete-ozone-layer/the-evolution-of-the-montreal-protocol

ozone, or in other words, the health effects that would have occurred if the ozone concentration that existed in 1979–1980 had been maintained through the time period modeled. The 1979–1980 concentrations of ozone are a common and widely used baseline for ozone concentrations and the benchmark concentration for ozone layer recovery (WMO, 2018). The AHEF consists of a series of independent sub-models (e.g., emissions, ozone projections, exposure to UV radiation, health effects) that estimate U.S. health benefits related to reductions in ODS emissions.

The accuracy of the AHEF's predictions depends upon continual updating of its inputs and methodologies to reflect ongoing scientific advances since the AHEF's creation. To this end, the AHEF has been updated several times and undergone multiple peer reviews since its inception (see Box 1).

Box 1: Previous Updates and Peer Reviews of the AHEF

2003: The AHEF was significantly updated in 2003 to incorporate new data and findings from various research projects. These revisions included: (1) recalibrated and refined stratospheric ozone concentration measurements; (2) improved forecasts of the impact of changing ozone concentrations on UV radiation intensity at the Earth's surface; (3) updated information on the biological effects of UV radiation of different wavelengths (action spectra), and how age and year of birth affect the induction of skin cancers and other human health effects; (4) improved estimation of projected skin cancer mortality rates, based on more recent and reliable epidemiological data;
(5) removal of the cataract sub-model until an agreed upon dose-response relationship became available; and (6) updated population data. These updates were tested and presented in a peer-reviewed report (U.S. EPA, 2006).

2010: A 2010 peer-reviewed report extended the health effects analysis by reintroducing modeling cataract incidence, as an improved parameterization from the original model. The updates that enabled AHEF to model cataract incidence included updated information on the biological effects of UV radiation, including dose-response data by skin type and sex, and more recent epidemiological data (U.S. EPA, 2010).

2015: The 2015 peer-reviewed report implemented updates to the ODS emissions scenarios and assessed incremental changes in health effects between different scenarios, showing slight reductions in projected incidence and mortality as a result of more stringent production and consumption controls that resulted in lower emissions than previously modeled (U.S. EPA, 2015).

This update and peer-reviewed report follows on from previous updates to make improvements to the AHEF model. While the science underlying the AHEF remains largely unchanged, the AHEF now incorporates new research results, such as updated physico-chemical parameters, improved UV irradiance calculations and updated population data. The AHEF is a living model, designed with the ability to accept changes in any model input or assumption based on new scientific findings, and/or to incorporate any new information as it becomes available. Despite these model updates, no model or set of results quantifying health effects impacts can be considered final, given that research on the atmospherics of ozone depletion and health effects of overexposure to UV radiation is ongoing. Many important issues must continue to be

investigated, and as significant new findings are incorporated into the AHEF, its estimates and the implications for protecting stratospheric ozone will be enhanced. In addition to the science updates, the AHEF code has been modernized to increase usability and flexibility, ensure compatibility with modern computing platforms, and enable custom modifications for future studies while ensuring no additional uncertainties have been introduced.

This report describes in detail each of these updates and provides an analysis of how these changes affect the health benefits estimated by the AHEF. With the current set of updates to the AHEF, the Montreal Protocol as amended and adjusted, compared with a scenario of no controls on ODS emissions, is now expected to prevent approximately 443 million cases of skin cancer, 2.3 million skin cancer deaths, and 63 million cataract cases for people in the United States born in the years 1890–2100.[2]

The remainder of this report is organized as follows:

- **Section II** presents updated modeling results for the Montreal Protocol scenarios.
- **Section III** provides an overview of the AHEF and recent updates by sub-model.
- **Section IV** suggests potential topics for future research.

These sections are followed by references and six appendices. Appendix A is a glossary of terms and Appendix B describes the ODS parameters in the AHEF model. Appendices C through E explore the sensitivity of the AHEF modeling assumptions, for future environmental and population conditions, early-life exposure weighting, and racial mapping to skin type. Appendix F models the incremental health effects of increased emissions of CFC-11.

II. Updated Results

II.1 Health Effects Results

This section first provides an overview of estimating human health effects in the AHEF and then compares historical U.S. melanoma incidence and mortality with modeled results from the updated AHEF. Next it looks at the modeled health benefits associated with the Montreal Protocol scenarios.

II.1.1 Overview of Human Health Effects Estimated in the AHEF

UV radiation-induced health effects are primarily related to the skin, eyes, and immune system. Skin effects include erythema (sunburn), aging of the skin, and various types of skin cancer: melanoma, squamous cell carcinoma, and basal cell carcinoma. Eye effects can include cataract, squamous cell carcinoma of the cornea and/or conjunctiva, and other damage to the surface of the eye. Overexposure to UV radiation can also reduce immunological defenses, which can result in the reactivation of latent viral infections, the strengthening of skin cancers caused by viruses, and increasing risks of infection (EEAP, 2019). Of the human health effects

[2] The AHEF calculates cumulative lifetime exposure to UV radiation of individuals beginning in 1980; thus, calculations begin with the 1890 birth cohort, assuming a 90-year lifespan.

from sun exposure, melanoma is the most lethal, causing nearly 7,000 deaths annually in the United States (American Cancer Society, 2020).

The health effects sub-model in the AHEF determines the change in incidence that will occur based on a relative change in UV radiation dosage (e.g., the number of health effect cases that occur as a result of comparing two policy scenarios, or a policy scenario compared with the 1979–1980 baseline conditions). While the health effects sub-model calculates baseline incidence uniformly across population groups, it uses updated biological amplification factors (BAFs) to investigate the health effect risks by skin type and sex.

The standard operating assumption in the AHEF is that individuals' sun exposure behavior remains the same in the scenario and baseline scenario. Human behavior to sun exposure is a source of uncertainty that is not easily quantified, so the AHEF assumes that human exposure behavior remains constant through time and does not explicitly take into account innovations in sun protection technology (e.g., improved sunglasses and sunscreens), increased public awareness of the effects of overexposure to UV radiation, or increased sensitization to the need for early treatment of suspicious lesions. For a more robust discussion of quantified and unquantified uncertainty in the AHEF, see U.S. EPA (2006).[3]

Each of the human health effects estimated by the AHEF is briefly described below.

Cutaneous Malignant Melanoma (CMM) or "Melanoma": Cutaneous malignant melanoma is a potentially life-threatening disease that results from the malignant transformation of skin cells called melanocytes, the melanin-producing cells found in the outer layer of the skin (called the epidermis or basal layer). Also referred to as "melanoma" in this report, cutaneous malignant melanoma is the most serious type of skin cancer. It occurs most frequently in persons over age 40 with light complexion and hair color.

Keratinocyte Cancer (KC): Also known as non-melanoma skin cancers (NMSC), these are a group of skin cancers that excludes melanoma but includes basal cell carcinoma, squamous cell carcinoma, and several other rare types. Collectively, they tend to behave very differently from melanoma and are often treated with different methods. Basal cell carcinoma and squamous cell carcinoma cancers originate from keratinocyte cells of the epidermis and rarely spread to other parts of the body.

Basal cell carcinoma is the most common type of skin cancer. It is caused primarily by exposure to UV radiation and occurs most frequently among light-skinned persons over age 45. Although basal cell carcinoma has a very high cure rate, in rare instances it can be lethal.

Squamous cell carcinoma is the second most common form of keratinocyte skin cancer in humans. It begins in the cells in the outer part of the skin and is thought to be primarily

[3] Human exposure behavior is a source of uncertainty that is not easily quantified. Estimates of incremental health effects will be less sensitive to behavioral changes over time, since these may "cancel out," as long as those changes are expected to occur in both the baseline and policy scenarios. Behavioral changes over time, however, will affect absolute estimates of health effect incidence and mortality.

caused by exposure to UV radiation. Squamous cell carcinoma may grow quickly and spread to other parts of the body, making it a dangerous form of skin cancer.

Cataract. Cataract is a clouding of the eye's naturally clear lens, which can cause vision impairment and blindness. Age-related cataract has a number of potential causes, but lifelong exposure to UV radiation, especially medium-wavelength UV-B rays, can play a significant role. There are three forms of cataract (nuclear, posterior subcapsular, and cortical), but only cortical cataract is clearly associated with exposure to UV radiation; much uncertainty exists with regard to the role of UV-B rays and the other forms of cataract.[4]

II.1.2 Comparison with Historical Health Effects

Total U.S. health effects calculated with the AHEF for a five-year period around 2010 are presented in Table 1.[5] For comparison purposes, Table 1 includes data from two sources: 1) the U.S. Department of Health and Human Services (DHHS), which reported 5-year means of melanoma incidence (for 2006–2010) and melanoma mortality (2007–2011) from aggregated data in reports to the U.S. National Cancer Institute and the U.S. Centers for Disease Control and Prevention (U.S. DHHS, 2014), and 2) the Institute for Health Metrics and Evaluation at University of Washington (IHME, 2017), which estimates annual incidence and mortality for melanoma and mortality for squamous cell carcinoma based on estimates from multiple studies. The DHHS data cover about 99.1 percent of the U.S. population, but do not include data on incidence or mortality estimates for keratinocyte cancer. The IHME data is included for comparison with AHEF squamous cell carcinoma mortality. IHME data for melanoma incidence and mortality show agreement with DHHS data despite using a different methodology. This increases confidence in the IHME data as an appropriate data source for a comparison against the AHEF results.

As shown in Table 1, the average annual melanoma incidence modeled from AHEF for the five-year period is 70,000 cases, while the observed incidences are 63,000 from DHHS and 71,000 from IHME. Of these 70,000 estimated cases, AHEF estimates 36,000 cases are in males and 34,000 cases are in females, while the observed incidences are 37,000 melanoma cases in males and 27,000 melanoma cases in females annually in the DHHS data set, and annual cases of 41,000 in males and 30,000 in females in the IHME data.

[4] The AHEF uses cataract baseline incidence estimates derived from computing annualized change as a function of age in prevalence data presented in Congdon et al. (2004). This study analyzed all three forms of cataract, but only cortical cataract is clearly associated with UV exposure. Thus, by using the Congdon et al. data to develop baseline cataract incidence in the AHEF, estimates given by AHEF and provided in this report are an upper bound of UV-induced cataract cases.

[5] These estimates assume the level of ODS emissions in the World Meteorological Organization (WMO) A1 scenario, as described in Box 2 further below.

Table 1. AHEF modeled annual average U.S. melanoma incidence (2007–2011) and mortality (2006–2010) compared with observational and modeled data

Health Effect	Data Source	Male	Female	Total
Melanoma Incidence 2007–2011	AHEF (modeled)	36,000	34,000	70,000
	DHHS (observed)	37,000	27,000	63,000
	IHME (modeled)	41,000	30,000	71,000
Melanoma Mortality 2006–2010	AHEF	4,900	3,300	8,200
	DHHS	5,800	3,000	8,800
	IHME	5,700	3,200	8,900
Squamous Cell Carcinoma Mortality 2006–2010*	AHEF	1,900	1,000	2,900
	IHME	2,100	900	3,000

Note: Totals may not sum due to independent rounding.
*Mortality reported in the AHEF is for all keratinocyte cancers; however, IHME only reports squamous cell carcinoma mortalities.

The average melanoma mortality modeled by the AHEF is 8,200 deaths per year, while the observed average mortality is 8,800 (DHHS) and 8,900 (IHME). The modeled 8,200 deaths comprise 4,900 in males and 3,300 in females, while the observed mortality is 5,800 in males and 3,000 in females from DHHS and 5,700 males and 3,200 females from IHME.

There are fewer data on keratinocyte cancer available to validate the AHEF modeling results, especially for incidence, because these cancers are not required to be reported to cancer registries. The IHME estimates the number of deaths from squamous cell carcinoma in the United States, totaling 2,951 deaths from 2006–2010, with 2,098 deaths of males and 853 of females. For this period, the AHEF estimates 2,941 deaths, with 1,892 deaths of males and 974 of females, from all keratinocyte cancer (i.e., both squamous cell carcinoma and basal cell carcinoma). Because squamous cell carcinoma is responsible for the majority of mortality associated with keratinocyte cancer (Rees, 2015), it is reasonable to use the estimates of squamous cell carcinoma mortality as a proxy for the mortality from all keratinocyte cancer. The fact that the AHEF does not separate mortality for squamous cell carcinoma and basal cell carcinoma, limited data for keratinocyte cancer mortality, and the dearth of observed incidence data for basal cell carcinoma in the United States prevent more direct comparisons.

Overall, the AHEF results show good agreement with the DHHS observational data, particularly considering that the data underlying the AHEF was gathered over two decades prior to the DHHS data. Similarly, the AHEF estimates for keratinocyte cancer mortality agree with the IHME estimates. The agreement reinforces confidence in the AHEF's projections of current and future health effects.

II.1.3 Health Benefits of the Montreal Protocol

The AHEF was used to calculate current and future health effects under the WMO A1 emissions scenario, corresponding to anticipated emissions under the Montreal Protocol as amended and adjusted (referred to as WMO A1).[6] The health effects presented below are U.S. "incremental" health effects, sometimes referred to as "excess" health effects, or the health effects associated with ozone depletion.[7] These cases are the difference in health effects between two modeled scenarios.

Box 2: Global ODS Emission Scenarios Used in This Report

Global ODS emissions scenarios have been developed on a compound-by-compound basis through the WMO ozone assessment process. As noted in Section **I.1**, "baseline" in this report refers to conditions pertaining to un-depleted ozone.

1. ***No Controls***

A "Business as Usual" scenario developed by the WMO (WMO, 2011) that envisages unregulated ODS emissions increasing continuously throughout the 21st century.

2. ***MP '87***

ODS emissions as anticipated under the Montreal Protocol on Substances that Deplete the Ozone Layer: the original landmark international agreement of 1987 (Velders et al., 2007; WMO, 2011).

3. ***WMO A1***

ODS emissions as anticipated under the Montreal Protocol as amended and adjusted (WMO, 2011), which adds chemicals to those covered by the original Protocol and also further regulates chemicals already covered by the original Protocol.

Estimates of future effects totals are extremely sensitive to assumptions about future conditions, and these estimates grow increasingly uncertain as environmental conditions and population projections evolve further from observed values. The extreme sensitivity of the "no controls" calculations to assumptions about the future and the selection of the end year for modeling is discussed in detail in Appendix C.

Given this uncertainty, health effect results are presented in this report in two ways. The first way (as shown in Section II.1.3.1) calculates health effects for people born in the birth cohorts of 1890 to 2100; this is the way that health effects have traditionally been presented in past AHEF reports. Note that the model estimates exposure and disease for groups of people born in five-year ranges centered on the year in the name of the cohort, so the 1890 cohort contains all Americans born 1888–1902, the 2100 cohort contains those born 2098–2102, and so on. Another way to present results (as shown in Section II.1.3.2) is to calculate health effects during the period 1980 to 2100. This approach yields lower estimates since it only calculates health effects occurring between 1980 and 2100, whereas the former approach includes health effects for much of the 22nd century, because individuals born in the later years of the time period live out their lives and continue to develop cancer and cataract during the 22nd century.

[6] This is referred to as the Montreal Protocol 2007 Scenario in the 2015 AHEF Report.

[7] "Incremental" effects are differentiated from "baseline" effects (those calculated for perpetual 1979–1980 ozone levels) and "total" effects, which are the absolute numbers of health effects anticipated under a given emissions scenario, i.e., the sum of "baseline" and "incremental" effects. See also Section III.5.

II.1.3.1 Health Effects for People Born in 1890–2100

Modeling by the updated AHEF shows that the WMO A1 scenario (full implementation of the Montreal Protocol as amended and adjusted), when compared with a scenario with no controls on ODS emissions, is expected to avoid 432 million cases of keratinocyte cancer and 11 million cases of melanoma, for a total of 443 million cases of skin cancer avoided in the United States during the lifetimes of people born in 1890 to 2100 (Table 2).[8] Over the same time period, it is estimated to avoid 800,000 deaths from keratinocyte cancer and 1.5 million from melanoma, for a total of 2.3 million skin cancer deaths. Further, it is expected to avoid 63 million cataract cases. To see the difference in UV radiation leading to the difference in health benefits between the original (1987) Montreal Protocol and the Montreal Protocol as amended and adjusted, see Appendix C (Figure C.1).

Table 2. Incremental U.S. health benefits of the Montreal Protocol as amended and adjusted (emissions scenario WMO A1) relative to no controls and to the original (1987) Montreal Protocol through the lifetimes of people born between 1890 and 2100

		Health effects avoided by Montreal Protocol as amended and adjusted, compared to no ODS controls	Additional health effects avoided by Montreal Protocol with amendments and adjustments relative to 1987 Montreal Protocol
Skin Cancer Incidence	Keratinocyte	432,000,000	230,000,000
	Melanoma	11,000,000	6,000,000
	Total	443,000,000	236,000,000
Skin Cancer Mortality	Keratinocyte	800,000	400,000
	Melanoma	1,500,000	800,000
	Total	2,300,000	1,300,000
Cataract Incidence		63,000,000	33,000,000

Note: Incidence estimates are rounded to the nearest million; mortality estimates are rounded to the nearest hundred thousand. Totals may not sum due to independent rounding.

II.1.3.2 Health Effects during the Period 1980–2100

During the period 1980–2100, the full implementation of the Montreal Protocol as amended and adjusted—compared with a scenario with no controls on ODS emissions—is expected to avoid 101 million cases of keratinocyte cancer and 3 million cases of melanoma, for a total of

[8] Birth years given in this report are the middle year of a 5-year cohort. Therefore, this population includes people born 1888–2102 to account for the first two years of the 1890 cohort and the last two years of the 2100 cohort.

104 million cases of skin cancer avoided in the United States. It is also estimated to avoid 170,000 deaths from keratinocyte cancer and 380,000 from melanoma, for a total of 550,000 skin cancer deaths in that time period. It is estimated to avoid 15 million cataract cases in the United States from 1980–2100 (Table 3).

The amendments and adjustments account for a significant portion of these health benefits over the original (1987) Montreal Protocol for people born in the United States, avoiding 38 million cases of keratinocyte cancer and 1 million cases of melanoma, totaling 39 million skin cancer cases avoided, through the year 2100. The Montreal Protocol as amended and adjusted is also estimated to avoid 60,000 deaths from keratinocyte cancer and 150,000 from melanoma, equaling 210,000 skin cancer deaths, as well as 5 million cataract cases avoided through the year 2100.

Table 3. Incremental U.S. health benefits of the Montreal Protocol as amended and adjusted (emissions scenario WMO A1) relative to no controls and to the original (1987) Montreal Protocol for years 1980–2100

		Health effects avoided by Montreal Protocol as amended and adjusted relative to no ODS controls	Additional health effects avoided by Montreal Protocol as amended and adjusted relative to 1987 Montreal Protocol
Skin Cancer Incidence	Keratinocyte	101,000,000	38,000,000
	Melanoma	3,000,000	1,000,000
	Total	104,000,000	39,000,000
Skin Cancer Mortality	Keratinocyte	170,000	60,000
	Melanoma	380,000	150,000
	Total	550,000	210,000
Cataract Incidence		15,000,000	5,000,000

Note: Incidence estimates are rounded to the nearest million; mortality estimates are rounded to the nearest ten thousand.

II.1.3.3 Annual Incremental Incidence of Health Effects

Figure 1 shows the U.S. annual incremental occurrence (that is, additional incidence and mortality attributable to ozone depletion) of the six health effects modeled by the AHEF under the WMO A1 ODS emissions scenario. Basal cell carcinoma has the highest peak incremental incidence (24,000 cases yr^{-1}), followed by squamous cell carcinoma incremental incidence (12,000 cases yr^{-1}), cataract incremental incidence (~5,000 cases yr^{-1}), melanoma incremental

incidence (1,000 cases yr^{-1}), melanoma mortality (130 deaths yr^{-1}), and keratinocyte cancer mortality (60 deaths yr^{-1}).

For the WMO A1 emissions scenario, the effects on stratospheric ozone of ODS emissions are assumed to have started in 1980 to align with the standard assumption of 1980 ozone concentrations as the baseline ozone condition. Therefore, modeled ozone depletion and increased exposure to UV radiation begin around 1980 and peak in the 1990s under the scenario, with stratospheric ozone projected to recover by the middle of the 21st century. Accordingly, the incremental health effects resulting from stratospheric ozone depletion begin to manifest in 1980. Health effect numbers are projected to peak several decades after peak ODS emissions since the manifestation of UV radiation-related biological damage occurs with a range of delay times owing to the need to accumulate UV radiation dosage over the course of a lifetime.[9] Similarly, projected health effects continue for some decades after ozone recovers to pre-1980 levels in the middle of this century. In fact, for the WMO A1 scenario, the AHEF predicts that some new cases will continue to occur beyond 2100, over 50 years after ozone recovery, because UV damage is cumulative, and patients will respond to exposure to UV radiation that they began accumulating in their youth.

The delay between peak Effective Equivalent Stratospheric Chlorine (EESC) and peak health effects shown in Figure 1 assumes that all exposure to UV radiation throughout a person's lifetime contributes equally to disease. However, delays in manifestation of some health effects may be longer than when modeled using cumulative lifetime exposure, as shown in Appendix D (U.S. EPA, 2006).

[9] The annual incremental effects, even at their peak, are a relatively small proportion of total U.S. health effects: e.g., the projected peak incremental melanoma incidence (~1000 cases yr-1 in 2036) is only 1.5% of the current (~2010) observed incidence of 63,000 (Table 1). This comparison, along with the "cases avoided" reported in Table 2 and Table 3, serves to illustrate the success of the Montreal Protocol as amended and adjusted.

Figure 1: U.S. annual incremental health effects for full implementation of the Montreal Protocol as Amended and Adjusted (WMO ODS emission scenario A1) relative to the "baseline" scenario with no ozone depletion (1980 ozone concentrations)

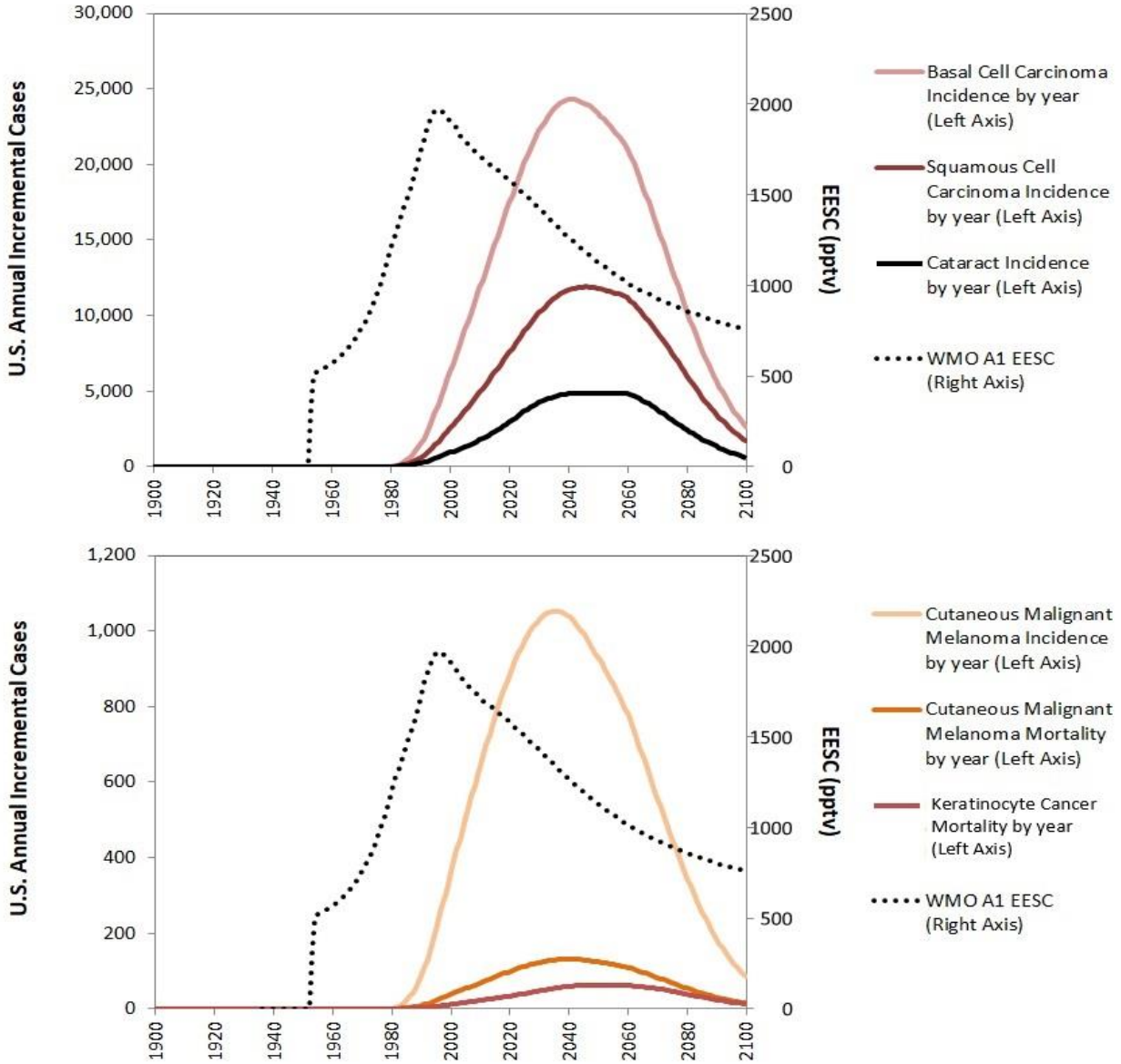

Figure 2 shows the relationship between peak ozone depletion and projected health effects similarly to Figure 1, except it plots health effects versus the birth year of the cohort developing the disease instead of the year the health effect occurs. For that reason, in this figure the health effects appear to peak to the left of (earlier than) the EESC peak. This is because cohorts born earlier than ozone depletion begins will be alive throughout the period of maximum exposure to UV radiation. Ozone depletion-related health effects begin to manifest in the 1920 birth cohort, i.e., those people who were approximately 60 years of age at the onset of ozone depletion. These early cohorts start with a smaller population than later cohorts, fewer of them are still alive by the time ozone depletion begins, and fewer still are alive after the delay between exposure to UV radiation and disease passes. For later birth years, a greater portion of their lives is lived under an ozone-depleted sky, and the onset of ozone depletion occurs when the cohort is younger, and more members are still alive.

The largest numbers of incremental health effects are manifested in the cohorts born between about 1960–2000. People in cohorts 1960–1980 experience the full period of ozone depletion and so receive the largest cumulative lifetime UV radiation doses. People born after 1980 are subject to progressively less cumulative incremental exposure to UV radiation as projected ozone levels return to 1980 levels during their lifetimes, leading to fewer total health effects.[10] Cohorts born in 2040 or later show no excess health effects above the baseline.

[10] One interesting feature of Figure 2 is that the 1980–1990 birth cohorts (spanning 1978–1992) show markedly higher incremental incidence than the immediately preceding cohorts. The additional peak for these birth cohorts results from the combination of three arithmetic factors: these cohorts, uniquely, experience the onset and acceleration of ozone depletion in their early childhood; the very youngest age groups are generally the largest at any given time; and, as noted above, the population steadily increases with time.

Figure 2: U.S. incremental health effects by birth cohort for successful implementation of the Montreal Protocol as Amended and Adjusted (WMO ODS emissions scenario A1, 2011) relative to the "baseline" scenario with no ozone depletion (1980 ozone concentrations)

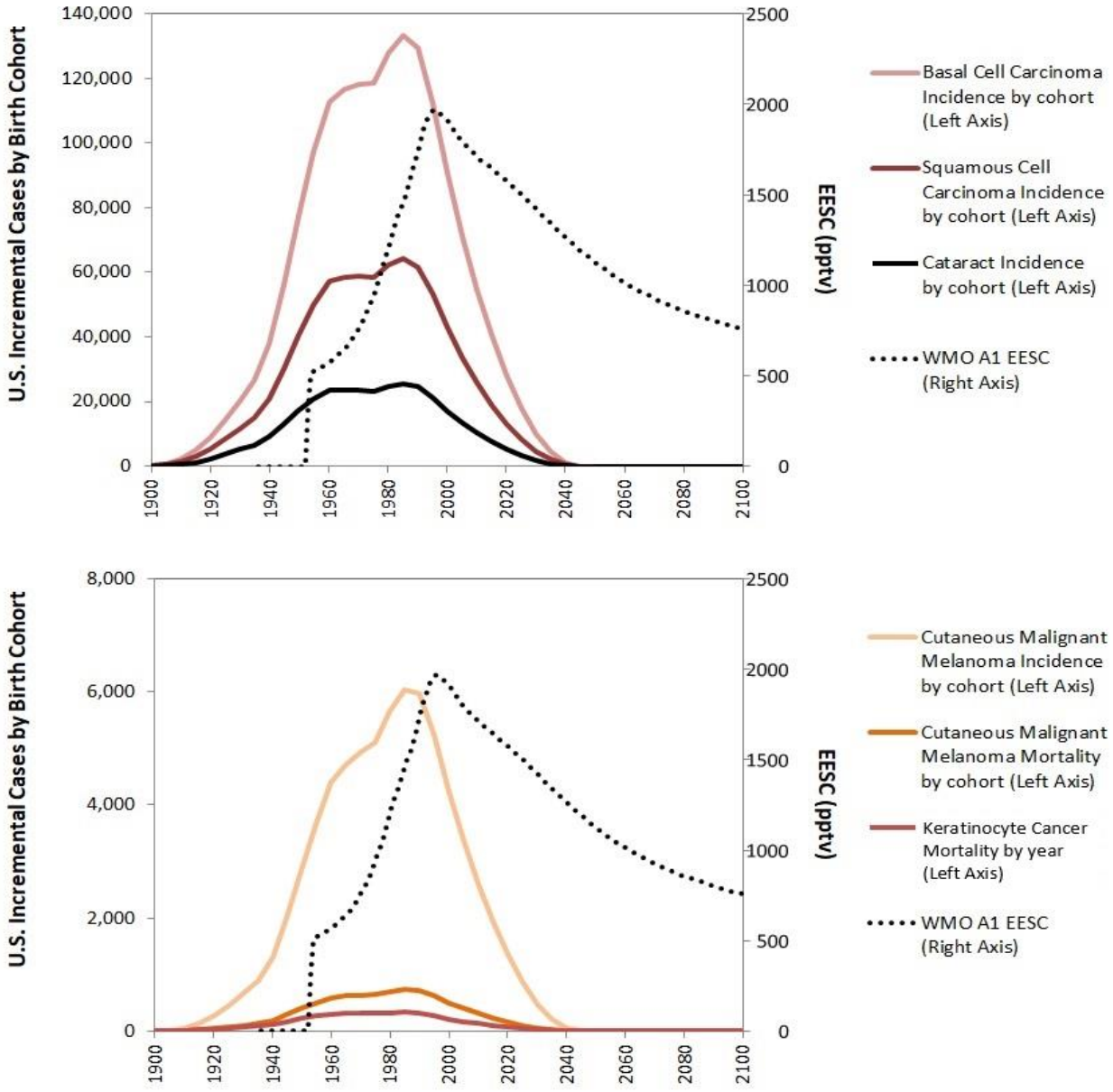

II.2 EESC and Ozone Results

In the 2019 update to the AHEF, recent research findings published since the last update of the AHEF were incorporated into the model. For example, global ODS emissions were corrected, adjusted, and expressed with more precision; the ODS species lifetimes (τ) were updated; and the 1980 baseline ozone value was reduced by approximately 0.1 percent. As shown by comparing the purple lines and the yellow dashed lines in Figure 3 and Figure 4, these updates produce only slight changes to the calculated EESC and ozone with respect to the most recent

previous version of the AHEF. The purple lines represent the WMO A1 scenario run in the AHEF before the current updates, while the yellow dashed lines represent the same scenario with the above updates but still using the 2010 stratospheric release factors for the ODS modeled. Stratospheric release factors are a molecular property of an ozone-depleting substance that are mostly derived through observation and are necessary to calculate EESC. Release factors describe the fraction of the halogen-carrying source gas that is photochemically lost as a function of mean age.

Stratospheric release factors were also updated based on the 2018 WMO report (WMO, 2018). The impact on calculated EESC and ozone can be seen by comparing the red and yellow dashed line in Figure 3 and Figure 4. As described above, the yellow dashed line was calculated using all of the current updates to the AHEF except the stratospheric release factors, and the red line was calculated with all of the updates including the 2018 stratospheric release factors. The updated factors used in the current report (red line) result in higher EESC than that calculated using the old release factors (yellow dashed line) by up to 2.3 percent after the year 2000. This minor change to the calculated EESC has only a small impact on the estimated health effects and produces estimates in good agreement with prior versions of the AHEF.

Figure 3: EESC for the WMO A1 emissions scenario

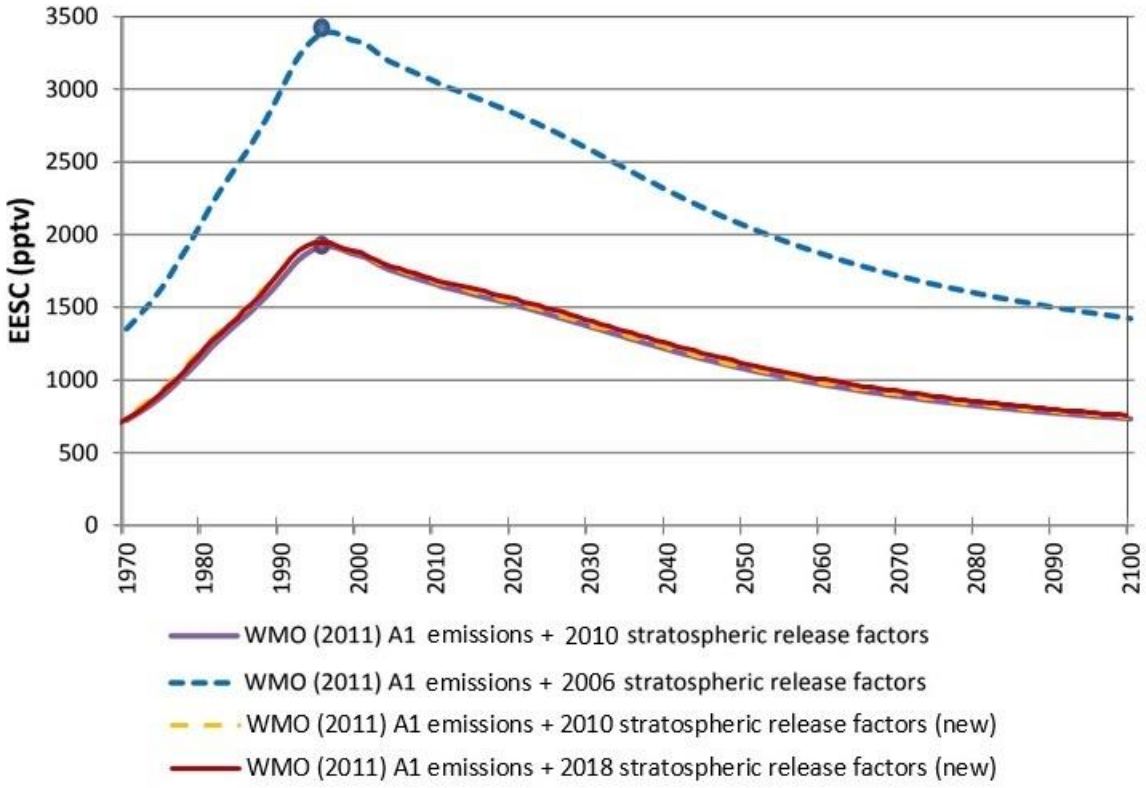

Note: Purple solid and blue dashed lines are the recommended and historic results, respectively, from U.S. EPA (2015). Previous stratospheric release factors are from U.S. EPA (2006) and WMO (2011); current stratospheric release factors are from WMO (2018).

Figure 4 shows annual mean ozone at 40–50°N calculated for the WMO A1 emissions scenario, using previous (U.S. EPA, 2006; WMO, 2011) and updated (WMO, 2018) ODS release factors. The ozone results from the 2015 report are also included here for reference (purple solid and blue dashed lines). Similarly to EESC, the calculated ozone has changed slightly since the values recommended in the 2015 AHEF report, with a projected recovery date of 2047. Comparing the yellow dashed and purple lines, we see that making all updates except the stratospheric release factors has little effect on calculated ozone concentrations or recovery date for the mid-latitude ozone layer. However, updating the stratospheric release factors as well, shown by the red line, leads to slightly lower modeled ozone concentration after 2000 and approximately a 3-year delay in a return to 1980 levels.

Figure 4: Annual mean ozone at 40–50°N for the WMO A1 emissions scenario

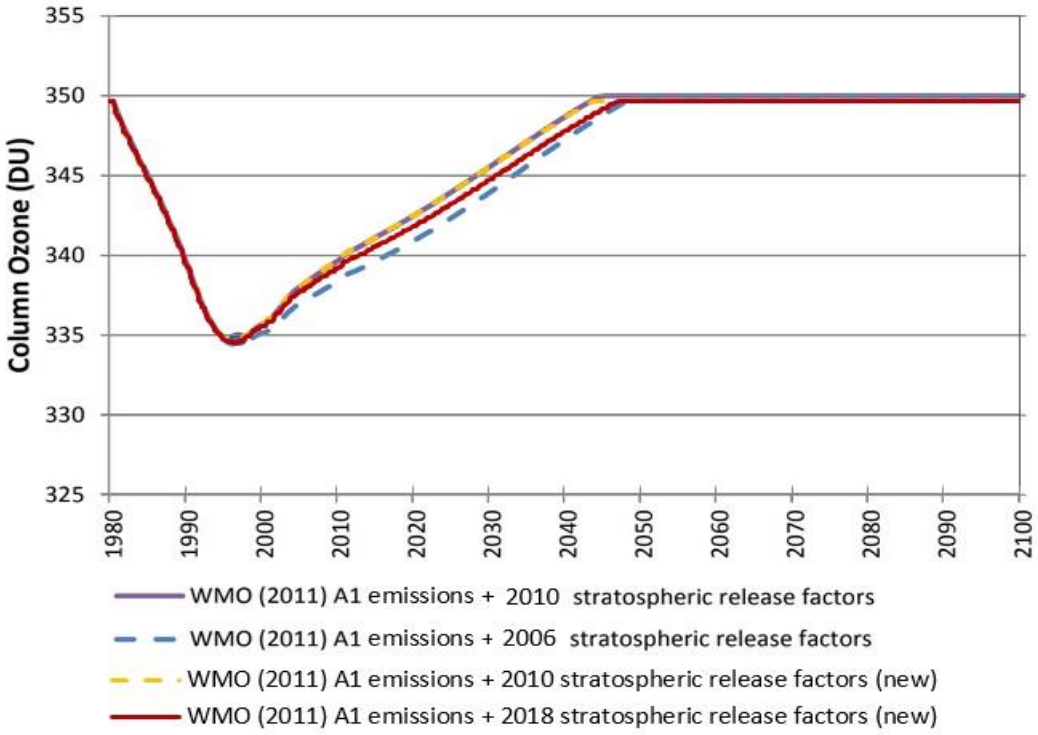

Note: Purple solid and blue dashed lines are the recommended and historic results, respectively, from U.S. EPA (2015). The differences between these two lines are far less for ozone than for EESC (Figure 3) because the ozone changes after 1980 are calibrated to deviations from the 1980 EESC value in each case, and not to the absolute EESC values (see Section III.2.1).

III. Model Overview and Updates

The AHEF has five main computational steps contained in sub-models that together calculate estimates for incidence and mortality for various UV radiation-related health effects for a given ODS emission scenario. The sub-model computations are as follows:

1. **Emissions Sub-model:** Simulates the past and future global emissions of 16 different ODS that are being phased out under the Montreal Protocol.
2. **Ozone Depletion Sub-model:** Models impacts of ODS emissions on stratospheric ozone via changes in stratospheric chlorine and bromine.
3. **UV Radiation Sub-model:** Models the induced instantaneous changes in ground-level UV radiation.
4. **Exposure Sub-model:** Models the cumulative personal exposure to UV radiation by year, age, and location.
5. **Effects Sub-model:** Derives dose-response relationships for incidence and mortality of health effects from baseline incidence data and projects changes in population-based future incidence and mortality.

The following discussion gives a brief summary of the existing methodology and describes the recent model updates. A schematic of the model is shown in Figure 5.

Figure 5: Overview of the AHEF Sub-models

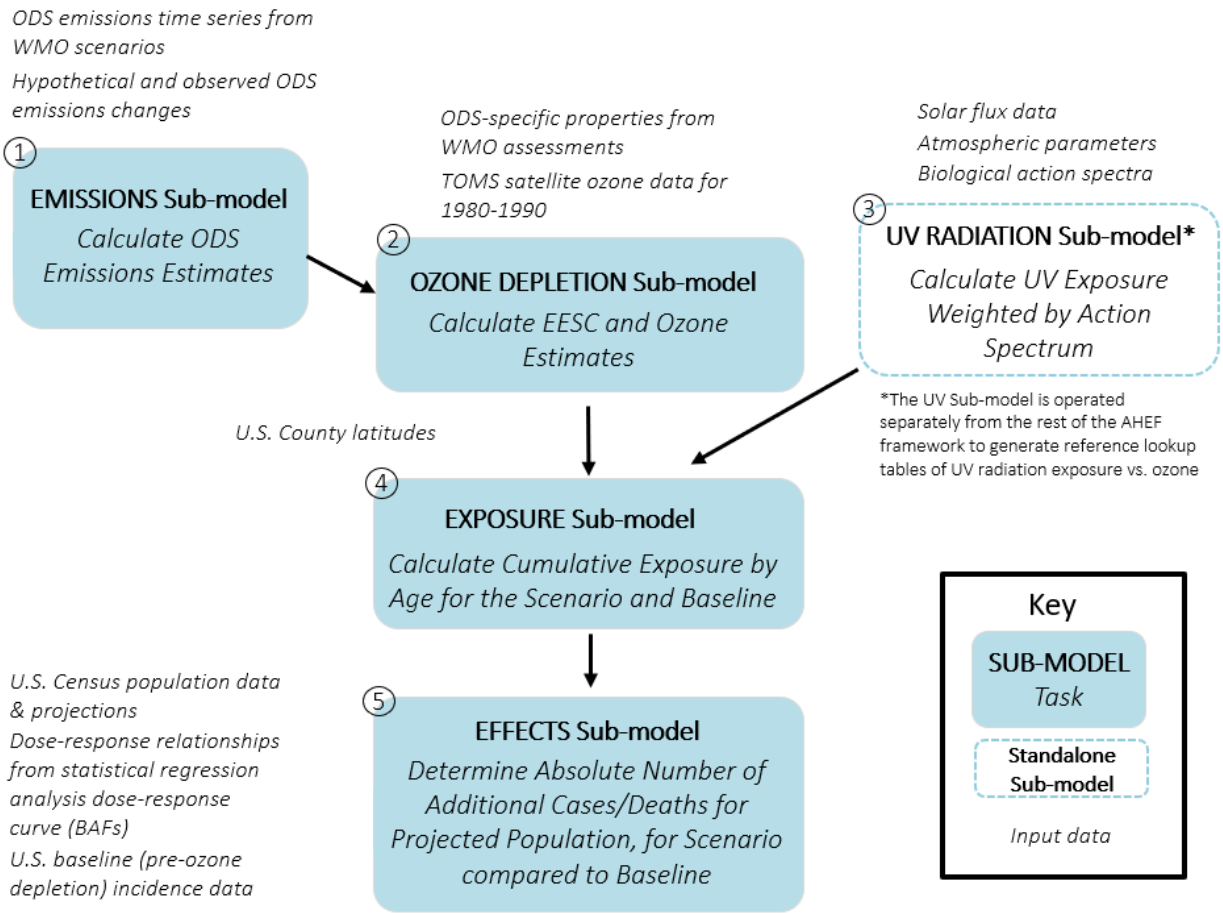

III.1 Emissions Sub-Model

III.1.1 Sub-model Description

The AHEF Emissions Sub-model describes the past and future global emissions of 16 different ODS that are being phased out under the Montreal Protocol. The Emissions Sub-model consists of two parts.

Part 1 comprises data tables of historical and future projected emissions, sourced from international reports. As noted in Box 2 above, the AHEF defines the "baseline" incidence and/or mortality for skin cancer and cataract as what would be expected to occur in the future if the concentration of stratospheric ozone remained fixed at 1979–1980 levels. This baseline provides a standard against which to evaluate increases in mortality and/or incidence for these health effects from future ODS emissions and ozone depletion and, under most scenarios, future recovery of the ozone layer to 1979–1980 levels. The WMO A1 emissions profile accounts for the 1987 Montreal Protocol and its associated amendments and adjustments through 2007. This dataset provides species-specific data at a global scale, is informed by observational data, provides ODS emissions estimates from 1950 to 2100, is compiled based on a number of recently developed international ODS datasets (as described below), and is globally recognized as representing the current state of the science.

The historical mixing ratios are from 1950 to 2009 and are derived from observations from NOAA and Advanced Global Atmospheric Gases Experiment (AGAGE) global sampling networks. For years before ongoing observations are available, the historical mixing ratio trends are derived from (1) when available, measured mixing ratios in firn-air samples,[11] and (2) modeled mixing ratios from consideration of industrial production magnitudes (e.g., the Alternative Fluorocarbons Environmental Acceptability Study[12]). The projected mixing ratios are based on production of ODS reported to the United Nations Environment Programme (UNEP), estimates of the bank sizes of ODS for 2008 from the Technology and Economic Assessment Panel; approved essential use exemptions for CFCs, critical-use exemptions for methyl bromide, and production estimates of methyl bromide for quarantine and pre-shipment use. When NOAA and AGAGE observations are available (this varies by species), the mixing ratio is an average of the two network observations.[13]

There is inherent uncertainty associated with data on ODS emissions, whether they are derived from top-down models, bottom-up models, or extrapolated from atmospheric measurements. The WMO 2010 assessment is no exception. All datasets are affected by uncertainty in emissions profiles and ODS characteristics, such as species lifetimes, transport of ODS to the stratosphere, composition of the future atmosphere, and other factors.

For the observational data used in the WMO dataset, there are uncertainties due to instrument calibration and modeling errors. That said, these independent sampling programs for

[11] Firn air sampling involves collecting samples of air trapped in the open pores of compacted snow that is left from previous seasons but has not yet been compacted into ice.
[12] https://agage.mit.edu/data/afeas-data
[13] See Table 5A-2 in the WMO (2011) report for detailed discussion of how the mixing ratio for each species was developed.

determining ODS global mixing ratios have improved substantially over time, with differences now typically on the order of a few percent or less (e.g., see Table 1-1 of WMO [2011]). In addition, there is uncertainty in the future bank projections that arises from estimates of the amount of material in the ODS bank reservoir and the rate at which the material leaks or is released from the bank.

Part 2 of the Emissions Sub-model is the computer code that provides the ability to modify the WMO emissions scenarios in a transparent way, in order to conduct "what-if?" calculations to explore the health impacts of hypothetical future emissions changes.

III.1.2 Updates

The updated AHEF model uses peer-reviewed, global ODS emissions tables for several different policy scenarios published by the WMO and UNEP quadrennial scientific assessments of ozone depletion (e.g., WMO, 2018), based on a synthesis and review of published research by the leading experts in stratospheric ozone science.

The Emissions Sub-model included in this updated version of the AHEF is completely new code. The input of emissions data has been standardized in the current version to facilitate the addition of new emissions scenarios as they become available. The new Emissions Sub-model allows users to adapt the input data tables to explore alternative future emissions scenarios and assess the effects on human health in the United States. A user can provide supplementary emissions files with annual global ODS emission increments (which may be positive or negative) for each of the 16 ODS species under consideration. The model then combines the standard and incremental emissions into a new modified global emissions file for use by the Ozone Depletion Sub-model. If an existing emissions file is used, the Emissions Sub-model code is not required.

III.2 Ozone Depletion Sub-model

III.2.1 Sub-model Description

The AHEF Ozone Depletion Sub-model projects impacts of past and future ODS emissions on stratospheric ozone. This sub-model estimates EESC and total column ozone for a given ODS emissions profile.

ODS such as chlorofluorocarbons, halons, carbon tetrachloride, methyl chloroform, methyl bromide, and HCFCs are used in a variety of applications including refrigeration and air-conditioning, foam blowing, aerosols, fire suppression and explosion protection, solvent cleaning, sterilants, adhesives, coatings, inks, and agricultural uses.

Some of these applications immediately emit the ODS used (e.g., fumigation and aerosols). Others emit the chemical as it performs a specific function over the course of a number of years. For example, the lifetime of some refrigeration equipment can be up to 25 years, some foams can continue emitting their blowing agent for up to 45 years, and fire suppression agents can remain in a total flooding system for years until discharged. As a result, new equipment production each year generates a stock of each chemical in those sectors with multi-year

emission profiles. This creates a time lag between initial use of some ODS and their subsequent emission into the atmosphere.

To model the ozone-depleting capacity of a certain concentration of ODS while accounting for the time delay between consumption and emission of the ODS, the AHEF estimates EESC. Specifically, the AHEF uses historical and projected global emissions and physico-chemical parameters of a suite of ODS to calculate time-varying stratospheric chlorine and bromine burdens, expressed as EESC. The methodology developed in the mid-1990s continues to be the appropriate approach for calculating EESC in the AHEF ozone sub-model, albeit updated to reflect current conditions.

First, the annual atmospheric ODS concentration is calculated by estimating ODS emissions "emitted" into the atmosphere and adding the concentration of the newly emitted ODS species to the concentration of the ODS species remaining in the atmosphere from the previous year. A three-year lag is assumed from the time ODS species are emitted to the time they reach the stratosphere. This procedure is repeated from 1950 to 2100. The estimate of each ODS species' concentration is integrated forward in time using the equation:

$$\text{ODS\_conc}(i, j) = \exp(-1/\tau_i) * \text{ODS\_conc}(i, j\text{-}1) + [1-\exp(-1/\tau_i)] * \tau_i * \text{ODS\_emis}(i, j) * F_{surf,i}$$

where

i = ODS molecule
j = year
ODS_conc(*i, j*) = atmospheric concentration of molecule *i* in year *j*
ODS_emis(*i, j*) = emission rate of molecule *i* in year *j*
τ_i = lifetime of molecule *i*
$F_{surf,i}$ = correction for vertical gradient (short-lived species only)

The annual EESC contribution of each ODS species is calculated by multiplying ODS_conc(*i,j*) by a stratospheric chlorine/bromine release factor and the number of reactive moieties associated with the ODS species (based on the fractional release rates). If the species is a brominated compound, then the product is multiplied by an additional factor (alpha) that represents the impact of bromine compared with chlorine in destroying stratospheric ozone. All EESC contributions are then summed for a global, annual EESC estimate.

In the previous equation, the first term of the right-hand side gives the contribution of the ODS remaining from emissions in previous years, while the second term gives the amount of ODS added, and partly removed, during the current year. The EESC for year j is then calculated from the equation:

$$\text{EESC}(j) = \sum_i \text{ODS\_conc}(i, j\text{-}3) * \text{Release Factor}(i) * (N_{Cl,i} + \alpha N_{Br,i})$$

where

Release Factor(*i*) = fraction of halogen released in the stratosphere by molecule *j*
$N_{Cl,i}$ and $N_{Br,i}$ = number of Cl and Br atoms in molecule *i*
j-3 = three-year delay representing transport from the troposphere to the stratosphere

The recovery of stratospheric ozone is nominally assumed to occur when EESC values no longer exceed those in the reference year, here taken as 1980. Thus, the following limit is applied:

$$EESC(j) = MAX[EESC(j), EESC(1980)]$$

This limit can optionally be bypassed, if considering scenarios that allow EESC values to fall below the 1980 value (i.e., if so-called ozone super-recovery is allowed).

Latitude-dependent time series of ozone (O_3) are then calculated by interpolating—and in many cases extrapolating—the correlation between EESC and ozone observed during the period 1980–1990. Specifically,

$$O_3(j, m, \text{lat}) = O_3(\text{Year1}, m, \text{lat}) + [A(m, \text{lat})/B] [EESC(j) – EESC(\text{Year1})]$$

where

j = year
m = month
lat = center of latitude band
Year1 = 1980
Year2 = 1990
$A(m, \text{lat}) = O_3(\text{Year2}, m, \text{lat}) – O_3(\text{Year1}, m, \text{lat})$
$B = EESC(\text{Year2}) – EESC(\text{Year1})$

The absolute values of the ozone column are not allowed to fall below 100 DU (which would occur only under catastrophic depletion scenarios):

$$O_3(j, m, \text{lat}) = MAX[100\ DU, O_3(j, m, \text{lat})]$$

The coefficient *A* was based on data from measurements obtained by the Total Ozone Mapping Spectrometer (TOMS). The coefficient *B* was found to be 438 parts per trillion by volume (ppt) per decade using the methodology above to estimate EESC under the WMO A1 scenario. Further, the B coefficient is now calculated for each AHEF simulation based on the EESC estimated specifically from a given emissions profile. The linear relationship described by the scaling equation above is considered to be reasonable for mid-latitudes, which experience relatively small ozone changes, unlike the Antarctic where an EESC threshold leads to non-linear ozone responses (WMO, 1999). For use in the AHEF, total column ozone values are restrained from dropping below 100 Dobson Units (DU), given this is far outside the range of any expected future mid-latitude values, or from exceeding the 1979–1980 baseline values.[14]

III.2.2 Updates

The physico-chemical parameters for individual ODS have been updated to values presented in the 2018 WMO report (see Table B.1 in Appendix B) (WMO, 2018). The lifetimes of ten ODS have been updated by factors varying between -50 percent (for CFC-115) and +40 percent (for Halon-2402). The global transport factors and ODS fractional chlorine release factors

[14] The AHEF baseline calculation, whereby ozone is maintained at its 1980 values, assumes that no ozone depletion had occurred before the period of TOMS satellite observations. This implies that 1) the EESC accumulated up to that point had no impact on stratospheric ozone, and 2) once EESC returns to the levels measured in 1980, stratospheric ozone will have completely recovered.

remain unchanged. The updates delay slightly the development of the net EESC profile, owing mainly to the increased lifetime of CFC-11, a major contributor to EESC in the early 21st century. The satellite observed EESC/O_3 relationship remains unaltered. The net result is that the calculated ozone time series is similar to previous results, with an ozone "recovery date" of 2047. In these calculations, once EESC returns to 1980 levels, the ozone recovery is frozen, as 1980 ozone levels are the generally accepted standard ozone baseline for exposure calculations. See Section II.2, *EESC and Ozone Results*, for comparison figures.

III.3 UV Radiation Sub-model

III.3.1 Sub-model Description

This section describes the method for calculating future ground-level UV irradiance and relating these values to changes in human health effects. First, the predicted future ozone concentrations under various policy scenarios (as discussed in the previous section) are used to model the change in UV radiation reaching the ground for the latitudes across the United States. Those predicted changes in ground-level UV radiation intensity are then biologically weighted using action spectra to reflect the extent to which different UV wavelengths cause a particular health effect (see Box 3).

Box 3: Biologically weighting UV radiation (Action Spectra)

An action spectrum describes the relative effectiveness of energy at different UV wavelengths in producing a particular biological response, such as development of melanoma, basal cell carcinoma, squamous cell carcinoma, or cataract. The AHEF and the Tropospheric Ultraviolet-Visible (TUV) model rely on action spectra for each health effect because action spectra provide information regarding which wavelengths of the total UV spectrum are most effective at causing the particular health effect. For example, UV-B wavelengths (280–320 nm) are known to cause erythema, as well as the development of skin cancer, cataract, and suppression of components of the immune system. UV-A radiation (320–400 nm) is not as readily absorbed by ozone (EEAP, 2019) and is not as potent as UV-B in the etiology of UV radiation damage-related health effects.

The AHEF uses the SCUP-h action spectrum (Spectrum Combined Utrecht/Philadelphia data, corrected for Human transmission) for modeling all types of skin cancer. The SCUP spectrum was derived on the basis of the induction of squamous cell carcinoma in hairless mice (denoted as SCUP-m). Because mouse skin and human skin have different absorption spectra for UV light, the action spectrum was corrected for human skin transmission by making adjustments to account for differences in epidermal thickness and the number of hair follicles per unit area. This adjusted action spectrum is denoted as SCUP-h (de Gruijl et al., 1993).

For cataract, the AHEF uses the Oriowo action spectrum due to both its coverage of optimum wavelengths and the similarity of the pig lens to the human lens in composition and UV response (Oriowo et al., 2001). The Oriowo action spectrum is based on the *in vitro* induction of cataract in whole, cultured pig lenses spanning across wavelengths from 270 to 370 nm, thus extending into the UV-A spectrum.

The UV Radiation Sub-model models the relationship between ozone and the amount of UV radiation reaching the Earth's surface using "look-up tables" generated with the Tropospheric Ultraviolet-Visible (TUV) atmospheric radiative transfer model. The TUV model

was developed and is maintained at the National Center for Atmospheric Research and is available at https://www2.acom.ucar.edu/modeling/tuv-download.

The TUV model first computes the amount of UV radiation reaching the Earth's surface as a function of solar zenith angle (SZA) and atmospheric composition including stratospheric ozone; this is done at each of 120 UV wavelengths from 280 to 400 nm. Next, the ground-level irradiance of each wavelength is multiplied by the biological effectiveness (action spectrum) of that wavelength and summed (integrated) over all contributing wavelengths, to yield the biologically effective irradiance. This is repeated over a grid of different solar angles and ozone columns, to generate a two-dimensional look-up table—one for each biological endpoint. The TUV model's look-up tables are interpolated in the AHEF to estimate exposure at different locations and times.

The calculation within the Exposure Sub-model of instantaneous biologically weighted UV irradiances can be summarized as:

$$UV\_Irradiance(O_3, SZA) \leftarrow \text{interpolation of lookup table}(O_3, SZA)$$

These values are calculated for each year *j*, each latitude band, and the 15th day of each month, then multiplied by 30 to obtain total monthly exposure doses.

III.3.2 Updates

The TUV model has undergone several updates between version 4.2/4.5 and the current version 5.4. These include a modernized solar spectrum at the top of the atmosphere, new high-resolution ozone absorption cross sections, and minor improvements to the numerical routines of the code.

The look-up tables were updated with the latest version of TUV (Version 5.4). The old tables for SCUP-h were calculated on 2 May 2003 using TUV version 4.2. The old tables for cataract were computed on 18 February 2009 using TUV4.5. While the differences between new and old tables are less than 2 percent, use of the new values ensures traceability to more recent versions of TUV.

III.4 Exposure Sub-model

III.4.1 Sub-model Description

An action spectrum describes the relative effectiveness of energy at different UV wavelengths in producing a particular biological response, such as development of melanoma, basal cell carcinoma, or squamous cell carcinoma. The AHEF and the TUV rely on action spectra for each health effect because action spectra provide information regarding which wavelengths of the total UV spectrum are most effective at causing the particular health effect. For example, UV-B wavelengths (280–320 nm) are known to cause erythema, as well as the development of skin cancer, cataract, and suppression of components of the immune system. UV-A radiation (320–400 nm) is not as readily absorbed by ozone (EEAP 2019) and is not as potent as UV-B in the etiology of UV radiation damage-related health effects. To ensure that the wavelengths are appropriately weighted when predicting each health effect, it is necessary to measure the extent to which wavelengths cause a particular health effect. Biologically weighted cumulative

exposure to UV radiation is calculated by the AHEF Exposure Sub-model for each U.S. county, year in the study period, and range of ages from 0–90 years old. The relevant weighted UV radiation dose for each month is interpolated from the tables generated by the TUV model. The doses are summed annually and then accumulated to yield age-dependent UV radiation dose estimates for each birth cohort, to cover all ages through the study period.

III.4.2 Updates

The UV radiation exposure calculation has been updated to use ozone interpolated to precise latitude (instead of using average ozone values for 10-degree latitude bands as done previously). This improvement results in a smooth north-south gradient in UV radiation exposure instead of the previous discontinuities between latitude bands. Data-type conflicts (real versus integer) have been resolved in the calculation of SZA, again resulting in more precise calculations. These changes impact the nationally aggregated effects calculations only incrementally since positive and negative changes in local UV radiation exposure tend to cancel out in the aggregated results.

III.5 Health Effects Sub-model

III.5.1 Sub-model Description

Once the appropriate action spectrum is selected for each health effect and the UV radiation dose of biologically active radiation and morbidity or mortality across latitudes are identified, statistical regression analyses are used to estimate the dose-response relationship, known as the BAF, for each health effect. The BAF measures the degree to which changes in exposure to UV radiation weighted by the appropriate action spectrum (as measured in Watts/m^2) cause incremental changes in health effects (incidence or mortality), estimated after accounting for the influence of birth year and age, as necessary.

BAFs are defined as the percent change in a health effect resulting from a one-percent change in the intensity of UV radiation (weighted by the chosen action spectrum). For each health effect, the AHEF applies the BAF to predict future incidence and mortality. Estimated ground-level effective UV irradiance from the TUV model is combined with a selected BAF to translate changes in exposure to UV radiation to a percentage change in expected health effects.

The Effects Sub-model uses previously defined dose-response relationships for health effect incidence and mortality and projects population-based future health effects and mortality changes. The health effects modeled include cutaneous malignant melanoma and keratinocyte cancer, along with its two main sub-types, basal cell carcinoma and squamous cell carcinoma, as well as cataract.

Several mathematical representations of the dose-response relationship are available within the AHEF, including exponential, power, and linear models.[15]

Response	~ $e^{a\ \mathrm{Dose}}$	(exponential)
	~ $(\mathrm{Dose})^{\mathrm{BAF}}$	(power)
ΔResponse/Response	= BAF (ΔDose/Dose)	(power, locally linear)

The last model (power, locally linear) is the default setting in the AHEF and corresponds most closely to the model used to represent epidemiologic data, i.e., the correlation over a significant latitude range of the observed incidence of a particular health effect with the measured or calculated exposure to UV radiation weighted for the same health effect. Specifically,

(Scenario Incidence) / (Baseline Incidence) =

1 + BAF x (relative change in cumulative UV exposure)

The BAFs have been determined for the health effects squamous cell carcinoma and basal cell carcinoma by de Gruijl and Forbes (1995), for melanoma for light-skinned males and females by Pitcher and Longstreth (1991) (see also U.S.EPA, 2006), and for cataract incidence by West et al. (1998; 2005). Tabulations of BAFs by sex, race, and health effect are used within the AHEF model, although cataract was found to be relatively insensitive to sex or race. Because evidence linking skin cancer incidence and mortality in dark-skinned populations is lacking or inconclusive, the AHEF only calculates these health effects for light-skinned groups. The EPA is not aware of any major updates to these relationships, and so these data remain unchanged in the current AHEF version. Should additional research on dose-response relationships or BAFs for endpoints modeled in the AHEF become available, the code has been modernized to allow simple substitutions for any new relationships.

The final step in the AHEF synthesizes all the data described above to estimate the current and future additional incidence of UV radiation-induced health effects for the U.S. population under various ODS emission scenarios. We define the following terms: “total” effects are the absolute numbers of health effects anticipated under a given emissions scenario and are the sum of “baseline” effects (those calculated for perpetual 1979–1980 ozone levels) and “incremental” effects (the additional health effects attributable to ozone depletion beyond 1979–1980 levels). The AHEF calculates cumulative lifetime exposure to UV radiation of individuals, thus calculations usually begin with the 1890 birth cohort, a few of whom survive into the period of

[15] The “power” and “exponential” models are two analytical functions commonly used to parameterize mildly non-linear data. The power model assumes that y (e.g., incidence) increases with x (e.g., exposure to UV radiation) according to the equation $y = a\ x^{b}$. For small changes (i.e., taking derivatives), it follows that $dy/y = b\ dx/x$. In other words, the relative (or percent) change in incidence is proportional to the relative UV change. The coefficient b is termed the Biological Amplification Factor (BAF) and is dimensionless. Correlations that fit this model are linear on a log-log plot, with slope b. An exponential model uses a form that explains how the relative change in incidence is proportional to the ***absolute*** change in exposure to UV radiation. The AHEF can use either power or exponential models, and either in their full non-linear form or linearized for small changes. The current default is the linearized power model.

ozone depletion. Calculations continue through 2100. The selection of calculation endpoint and its implications are discussed in detail in Appendix C.

III.5.2 Updates

Population data subdivided by race, sex, age, county, and year for the period up to 2100 are needed as input into the effects sub-model of the AHEF. Subdivided annual data were sourced from the U.S. Census Bureau for the period 1985–2018 (U.S. Census Bureau, 2016a; U.S. Census Bureau, 2016b; U.S. Census Bureau, 2017; and U.S. Census Bureau, 2019a). (Detailed data are not available prior to 1985, so the AHEF applies the 1985 values to all prior years.) The 1985–2018 data are an improvement from previous iterations of the AHEF, as previously these data were only available in 5-year increments through 1990.

Additionally, national population totals have been updated annually for the period 2019–2060 based on population projections from the U.S. Census Bureau (U.S. Census Bureau, 2019b). Previously national projections were only available in 5-year increments through 2050. The U.S. Census Bureau projections are subdivided by race, sex, age, and year, but not by county. Because of this, the model distributes these projected data among counties in proportion to the 2016 data distributions. We apply projections individually to each of six sub-populations listed by the U.S. Census Bureau: white male and female, black male and female, “other” male, and “other” female. The projected “white” and “other” populations are summed for the health effects calculation, in effect assuming that the rate of health effects in the “other” populations may be described by the data for “light-skinned” populations. A sensitivity study is presented in Appendix E, detailing the effects of this assumption. Projections are unavailable after 2060 so the population is assumed to remain constant between 2060 and 2100.

The updated census data led to significantly increased health effects totals over previous reports, since the population projections are greater than in previous datasets and are projected further into the 21st century.

IV. Potential Topics for Future Research

Because research on the health effects of exposure to UV radiation is ongoing, no model or set of results quantifying health effects impacts can be considered final. New information and research results on skin cancer and UV radiation continue to be generated. As significant new findings are incorporated into the AHEF, the accuracy of its estimates should be enhanced. However, it is clear that protecting the stratospheric ozone layer has profound benefits for human health.

Many important issues remain to be explored, such as the expansion of AHEF calculations to other geographies, calculation of fractional chlorine release, incorporation of research on other human health endpoints (e.g., immune suppression), and application of the AHEF to new scenarios such as non-compliance with the Montreal Protocol’s obligations. This section discusses some of the major topics where future research could improve the ability to accurately estimate UV radiation-related impacts and expand the scope and implications of the AHEF’s results.

IV.1 Other Geographies

The AHEF currently only models health benefits in the United States. However, there is interest in expanding the scope of the AHEF to other countries or areas of the world. From an operational standpoint, the code is flexible enough to allow such an expansion, although it is best suited for mid-latitudes in both the Northern and Southern Hemispheres; other latitudes would require different calibrations. The calculation would first require knowledge of the population characteristics and latitudinal distribution for the new geographical region. A user would modify the AHEF sub-model defining geographical parameters so that the AHEF could successfully read and use the new population and location files. Second, the AHEF would need data on health effect incidence and mortality for the new population(s) under consideration. Ideally, baseline incidence data (by age, gender, and race) would be available; if such data were not available, then baseline incidence could be estimated from correlations such as those shown in Xiang et al. (2014), based on location-specific UV estimates. BAFs derived from such correlations would need to be evaluated across different locations.

IV.2 Fractional Chlorine Release

The calculation of fractional chlorine release has recently been updated in another (more complex) model (Engel et al., 2018). These new values are based on new estimates of the time an ODS molecule spends in the stratosphere before being photo-dissociated or returned to the troposphere. The project team is exploring whether a simple parameterization of these updates is possible.

IV.3 Other Health Effect Relationships

The AHEF currently models skin cancer mortality, skin cancer incidence, and cataract incidence, but these are not the only health effects of increased exposure to UV-B radiation. For instance, UV-induced immune suppression can cause the reactivation of latent herpes viral infections, potentiate skin cancers caused by viruses such as human papilloma viruses (HPV), and increase risks of bacterial and protozoal infection (EEAP, 2019). Epidemiological studies have pointed to a correlation between exposure to UV-B and prevalence of HPV (Ramagosa, 2008; Chen et al., 2008; Hampras et al., 2014; Uberoi et al., 2016).

Conversely, changes in UV radiation may have implications for the risk of infection of vector-borne and water-borne diseases, since UV radiation is potentially insecticidal (EEAP, 2019). Similarly, recovery of stratospheric ozone, by reducing UV-B radiation, may contribute to a decrease in vitamin D production.

To enable AHEF modeling for other health effects, a systematic review of the evidence would be required to establish the causal relationship with exposure to UV radiation, which wavelengths contribute most (the action spectrum), and the sensitivity of the endpoint to the UV radiation dose (the dose-response relationship, as embodied in the BAF). While such data are still relatively sparse, the growing body of literature may soon enable these extensions within the AHEF.

IV.4 Non-compliance with Emissions Controls

The AHEF model is ideally suited to examine deviations from the expected phaseout of certain ODS, including the effects on global EESC, seasonal and latitudinal changes in stratospheric ozone and ground-level UV radiation, and estimates of associated health problems (melanoma and keratinocyte cancer, and cataract). For example, recent measurements of atmospheric concentrations suggest that CFC-11 has decreased at a rate slower than expected under full compliance with the Montreal Protocol (Montzka et al., 2018; Rigby et al., 2019). The corresponding emission anomalies can be added to the AHEF standard scenarios to quantify the incremental health disbenefits (see Appendix F on estimating the impact of increased emissions of CFC-11).

References

American Cancer Society (2020). Melanoma of the skin. Available online at: https://cancerstatisticscenter.cancer.org/?_ga=2.215799443.521518943.1574698802-1090167468.1574698802#!/cancer-site/Melanoma%20of%20the%20skin. (Accessed on March 2, 2020)

Chen, A.C., N.A.J. McMillan, and A. Antonsson (2008). Human papillomavirus type spectrum in normal skin of individuals with or without a history of frequent sun exposure. *J Gen Virol, 89*: 2891–2897. doi: 10.1099/vir.0.2008/003665-0

Congdon et al. (2004). Prevalence of cataract and pseudophakia/aphakia among adults in the United States. *Archives of Ophthalmology, 122:* 487–494.

de Gruijl, F.R. and P.D. Forbes (1995). UV-induced skin cancer in a hairless mouse model. *BioEssays, 17*: 651–660.

de Gruijl, F.R., H.J. Sterenborg, P.D. Forbes, R.E. Davies, C. Cole, G. Kelfkens, H. van Weelden, H. Slaper, and J.C. van der Leun (1993). Wavelength dependence of skin cancer induction by ultraviolet irradiation of albino hairless mice. *Cancer Research, 53*: 53–60.

Dhomse, S.S., Feng, W., Montzka, S.A. et al. (2019). Delay in recovery of the Antarctic ozone hole from unexpected CFC-11 emissions. *Nature Communications*, 10 (5781). doi: 10.1038/s41467-019-13717

Environmental Effects Assessment Panel (EEAP) (2019). Environmental Effects and Interactions of Stratospheric Ozone Depletion, UV Radiation, and Climate Change. 2018 Assessment Report. Nairobi: Environmental Effects Assessment Panel, United Nations Environment Programme (UNEP). Available online at: https://ozone.unep.org/science/assessment/eeap. (Accessed on March 2, 2020)

Engel, A., H. Bönisch, J. Ostermöller, M. P. Chipperfield, S. Dhomse, and P. Jöckel (2018). A refined method for calculating equivalent effective stratospheric chlorine. *Atmos. Chem. Phys.*, *18*: 601–619. doi: 10.5194/acp-18-601-2018

Geller, A.C., et al. (1998). Do pediatricians counsel families about sun protection? *Archives of Pediatric and Adolescent Medicine, 152*: 372–376.

Hampras S.S., A.R. Giuliano, H.Y. Lin, K.J. Fisher, M.E. Abrahamsen, B.A. Sirak, M.R. Iannacone, T. Gheit, M. Tommasino, and D.E. Rollison. (2014). Natural history of cutaneous human papillomavirus (HPV) infection in men: the HIM study. *PLoS One, 9*(9): e104843. doi: 10.1371/ journal.pone.0104843

Harrison, S.L., R. MacLennan, R. Speare, and I. Wronski (1994). Sun exposure and melanocytic naevi in young children in Townsville, Queensland. *Lancet*, *344*: 1529–1532.

Institute for Health Metrics and Evaluation (IHME) (2017). Global Burden of Disease Results Tool. Available online at: http://ghdx.healthdata.org/gbd-results-tool. (Accessed February 4, 2020)

Montzka, S.A., G.S. Dutton, P. Yu, E. Ray, R.W. Portmann, J.S. Daniel, L. Kuijpers, B.D. Hall, D. Mondeel, C. Siso, J.D. Nance, M. Rigby, A.J. Manning, L. Hu, F. Moore, B.R. Miller, and J.W. Elkins (2018). An unexpected and persistent increase in global emissions of ozone-depleting CFC-11. *Nature*, *557*: 413–417. doi:10.1038/s41586-018-0106-2

Oriowo, O.M., A.P. Cullen, B.R. Chou, and J.G. Sivak (2001). Action spectrum and recovery for in vitro UV-induced cataract using whole lenses. *Investigative Ophthalmology & Visual Science*, *42*: 2596–2602.

Pitcher, H.M., and J.D. Longstreth (1991). Melanoma mortality and exposure to ultraviolet radiation: an empirical relationship. *Environment International, 17*: 7–21.

Ramagosa, R., E.M. de Villiers, J.E. Fitzpatrick, and R.P. Dellavalle (2008). Human papillomavirus infection and ultraviolet light exposure as epidermoid inclusion cyst risk factors in a patient with epidermodysplasia verruciformis? *Journal of the American Academy of Dermatology*, *58*(5 Suppl 1): S68.e1–6. Available online at: https://www.ncbi.nlm.nih.gov/pmc/articles/PMC2587233/. (Accessed on March 2, 2020)

Rees, J.R., M.S. Zens, M.O Celaya, B.L Riddle, M.R. Karagas, and J.L. Peacock (2015). Survival after squamous cell and basal cell carcinoma of the skin: A retrospective cohort analysis. *Int J Cancer*. 137(4): 878–884. doi:10.1002/ijc.29436

Rigby, M., S. Park, T. Saito, L.M, Western, A.L. Redington, X. Fang, S. Henne, A.J. Manning, R.G. Prinn, G.S. Dutton, P.J. Fraser, A.L. Ganesan, B.D. Hall, C.M. Harth, J. Kim, K.-R. Kim, P.B. Krummel, T. Lee, S. Li, Q. Liang, M.F. Lunt, S.A. Montzka, J. Muhle, S. O'Doherty, M.-K. Park, S. Reimann, P.K. Salameh, P. Simmonds, R.L. Tunnicliffe, R.F. Weiss, Y. Yokouchi, and D. Young (2019). Increase in CFC-11 emissions from eastern China based on atmospheric observations. *Nature*, *569*: 546–550, doi: 10.1038/s41586-019-1193-4.

Uberoi, A., S., Yoshida, I.H. Frazer, H.C. Pitot, and P.F. Lambert (2016). Role of ultraviolet radiation. Ultraviolet Radiation in Papillomavirus-Induced Disease. *PLoS Pathogens, 12*(5): e1005664. doi:10.1371/journal.ppat.1005664

United Nations Environment Programme (UNEP) (2019). All about Ozone and the Ozone Layer. United Nations Environment Programme. Available online at: https://ozone.unep.org/ozone-and-you. (Accessed on March 2, 2020)

U.S. Census Bureau (2016a). Intercensal County Estimates by Age, Sex, Race: 1980–1989. Available online at: https://www.census.gov/data/datasets/time-series/demo/popest/1980s-county.html. (Accessed on March 2, 2020)

U.S. Census Bureau (2016b). Intercensal Estimates of the Resident Population by Five-Year Age Groups, Sex, Race, and Hispanic Origin for Counties: April 1, 2000 to July 1, 2010. Available online at: https://www.census.gov/data/datasets/time-series/demo/popest/intercensal-2000-2010-counties.html. (Accessed on March 2, 2020)

U.S. Census Bureau (2017). State and County Intercensal Datasets: 1990–2000. Available online at: https://www.census.gov/data/datasets/time-series/demo/popest/intercensal-1990-2000-state-and-county-characteristics.html. (Accessed on March 2, 2020)

U.S. Census Bureau (2019a). Annual County Resident Population Estimates by Age, Sex, Race, and Hispanic Origin: April 1, 2010 to July 1, 2018. Available online at: https://www2.census.gov/programs-surveys/popest/datasets/2010-2018/counties/asrh/cc-est2018-alldata.csv?# . (Accessed on March 2, 2020)

U.S. Census Bureau (2019b). 2018 National Population Projections Tables: Race and Hispanic Origin by Age Group. Available online at: https://www.census.gov/data/datasets/2017/demo/popproj/2017-popproj.html. (Accessed on March 2, 2020)

U.S. Department of Health and Human Services (U.S. DHHS) (2014). The Surgeon General's call to action to prevent skin cancer. Washington, D.C.: U.S. Dept of Health and Human Services, Office of the Surgeon General. Available online at: https://www.surgeongeneral.gov/library/calls/prevent-skin-cancer/index.html. (Accessed on March 2, 2020)

U.S. EPA. (2006). Human Health Benefits of Stratospheric Ozone Protection. Available online at: https://cfpub.epa.gov/si/si_public_record_report.cfm?Lab=OAP&dirEntryId=73966. (Accessed on March 2, 2020)

U.S. EPA. (2010). Protecting the Ozone Layer Protects Eyesight: A Report on Cataract Incidence in the United States Using the AHEF Model. Available online at: https://rfflibrary.wordpress.com/2010/08/02/protecting-the-ozone-layer-protects-eyesight-a-report-on-cataract-incidence-in-the-united-states-using-the-atmospheric-and-health-effects-framework-model/. (Accessed on March 2, 2020)

U.S. EPA. (2015). Updating Ozone Calculations and Emissions Profiles for Use in the Atmospheric and Health Effects Framework. Available online at: https://www.epa.gov/sites/production/files/2015-07/documents/updating_ozone_calculations_and_emissions_profiles_for_use_in_the_atmospheric_and_health_effects_framework_model.pdf. (Accessed on March 2, 2020)

U.S. EPA. (2019). International Treaties and Cooperation about the Protection of the Stratospheric Ozone Layer. Available online at: https://www.epa.gov/ozone-layer-protection/international-treaties-and-cooperation-about-protection-stratospheric-ozone. (Accessed on March 2, 2020)

Velders G.J.M., S.O. Andersen, J.S. Daniel, D.W. Fahey, and M. McFarland (2007). The importance of the Montreal Protocol in protecting climate. *Proceedings of the National Academy of Sciences of the United States of America*, 104(12): 4814–4819.

West, S., D. Duncan, B. Muñoz, G. Rubin, L. Fried, K. Banden-Rouche, and O. Schein (1998). Sunlight exposure and risk of lens opacities in a population-based study: The Salisbury Eye Evaluation Project. *Journal of the American Medical Association*, 280: 714–718.

West, S., J. Longstreth, B. Muñoz, H. Pitcher, and D. Duncan (2005). Model of risk of cortical cataract in the U.S. population with exposure to increased ultraviolet radiation due to stratospheric ozone depletion. *American Journal of Epidemiology*, 162: 1080–1088.

WMO (World Meteorological Organization) (2018). Executive Summary: Scientific Assessment of Ozone Depletion: 2018. *Global Ozone Research and Monitoring Project – Report No. 58*: 67, Geneva, Switzerland.

WMO (2014). Assessment for Decision-Makers: Scientific Assessment of Ozone Depletion: 2014. *Global Ozone Research and Monitoring Project—Report No. 56*: 88, Geneva, Switzerland.

WMO (2011). Scientific Assessment of Ozone Depletion: 2010. *Global Ozone Research and Monitoring Project – Report No. 52*: 516, Geneva, Switzerland.

WMO (1999), Scientific Assessment of Ozone Depletion: 1998. *World Meteorological Organization Global Ozone Research and Monitoring Project -- Report No. 44*. Geneva, Switzerland.

Xiang, F., R. Lucas, S. Hales, and R. Neale (2014). Incidence of nonmelanoma skin cancer in relation to ambient UV radiation in white populations, 1978–2012: empirical relationships. *JAMA Dermatol., 150*(10): 1063–1071.

Zanetti, R., S. Franceschi, S. Rosso, S. Colonna, and E. Bidoli (1992). Cutaneous melanoma and sunburns in childhood in a southern European population. *European Journal of Cancer*, *28A*: 1172–1176.

Appendix A. Glossary and Acronyms

Action spectrum — Experimentally-derived plots describing the relative effectiveness of each wavelength of UV-A and UV-B radiation in the induction of a specific health effect (e.g., skin cancer, sunburn). Action spectra are used as weighting functions in order to estimate the potential of a particular exposure to UV radiation to induce adverse health effects.

Biological amplification factor (BAF) — BAFs are equal to the slope of the dose-response curve (see "dose-response relationship").

Basal cell carcinoma (BCC) — Basal cell carcinoma is the most common type of skin cancer. It begins in the cells in the inner part of the skin, is caused primarily by exposure to ultraviolet radiation, and occurs most frequently among light-skinned persons over age 45. Although basal cell carcinoma has a very high cure rate, in rare instances it can be lethal.

Baseline — The AHEF defines the "baseline" incidence and/or mortality for skin cancer and incidence of cataract as what would be expected to occur in the future if the concentration of stratospheric ozone remained fixed at 1979–1980 levels.

Birth cohorts — Individuals assigned by year of birth into groups of five years for further study. The AHEF uses the results of these birth cohort studies to create and project a baseline estimate of skin cancer incidence and/or mortality and cataract incidence. When birth years are referenced in this report, the year given is the middle year of the 5-year span of the cohort, e.g., 1890–2100 includes individuals born from 1888 through 2102.

Column ozone — The amount of ozone (measured in Dobson units) contained in a vertical column of air extending from the Earth's surface to an orbiting satellite designed to measure ozone concentrations. Roughly 90 to 95 percent of column ozone is in the stratosphere with small amounts (5–10 percent) in the troposphere.

Cutaneous malignant melanoma (CMM) — Also referred to as "melanoma" in this report, cutaneous malignant melanoma is the most serious type of skin cancer. It occurs most frequently in light-skinned persons over age 40 with light complexions and hair color. It begins in the melanocytes, the skin's melanin-producing cells.

Dobson unit (DU) — A measure of the thickness of the ozone. For a vertical column of ozone compressed at 0 degrees Celsius and 1 atmosphere pressure, a Dobson unit is defined to be 0.01 millimeter thick.

Dose metrics — Measures used to express the amount of UV radiation received over a specific time period (i.e., the dose). Examples are peak hour dose, daily dose, or cumulative doses for a month or for an entire year.

Dose-response relationship — The relationship between an effect, or response (e.g., skin cancer), and the exposure, or dose (e.g., UV radiation), producing that effect. If plotted on a log-log scale, BAFs are equal to the slope of the dose-response curve.

Econometric — A statistical technique that enables analysts to determine to what degree one specific variable (e.g., exposure to UV radiation) may be responsible for a specific effect (e.g., skin cancer) thought to be caused by the interaction of several related variables. For example, it is hypothesized that age, birth year, and exposure to UV radiation all play a role in

the etiology of melanoma. Because ODS control policies can only reduce one of these risk factors (i.e., the amount of UV-B reaching the ground can be reduced by a thicker ozone layer), econometric estimation is used to isolate and quantify the contribution of exposure to UV radiation to melanoma incidence and mortality.

Equivalent effective stratospheric chlorine (EESC) — EESC is a metric for representing ODS levels in the stratosphere. The EESC of substances that contain bromine instead of chlorine can be calculated by using a bromine efficiency factor ("alpha factor") that defines the number of chlorine molecules needed to deplete one molecule of ozone as efficiently as one bromine molecule. The AHEF assumes that 60 chlorine molecules are needed to deplete a molecule of ozone as efficiently as one bromine molecule. It is calculated based upon three factors: surface atmospheric concentrations of individual ODS and their number of chlorine and bromine atoms, the relative efficiency of chlorine and bromine for ozone depletion, and the time required for the substances to reach different stratospheric regions and break down to release their chlorine and bromine atoms.

Incidence — For the purposes of this paper, the incidence is defined as the number of new cases of a given health effect that develop each year.

Isotropic ground reflectivity — The assumption that all wavebands of UV radiation striking the Earth's surface are reflected equally in all directions.

Keratinocyte cancer (KC) — Also known as non-melanoma skin cancer (NMSC), this is a group of skin cancers that excludes melanoma but includes squamous cell carcinoma, basal cell carcinoma, and several other rare types. Collectively, they tend to behave very differently from melanoma and are often treated with different methods.

Latency — The length of time between the exposure to a stressor (e.g., UV-B radiation) and the response to that stressor (e.g., skin cancer).

Montreal Protocol — *The Montreal Protocol on Substances that Deplete the Ozone Layer* is a global agreement to protect the Earth's ozone layer by phasing out the chemicals that deplete it.

No super-recovery — The total column ozone observed in the 1979–1980 timeframe is defined as the baseline against which the impacts of future ozone changes are measured. These column ozone levels are assumed in the AHEF to remain constant in the baseline projections.

Ozone-depleting substances (ODS) — Manmade chemicals containing halogens that destroy ozone molecules in the stratosphere. Emissions of these chemicals are the main cause of stratospheric ozone depletion and many ODS have been targeted for phaseout by the Montreal Protocol and its amendments (UNEP, 2019).

Prevalence — Refers to the total number of existing cases of a given health effect at a specific time, as opposed to new cases ("incidence").

Solar UV irradiance — The total energy of UV radiation from the sun reaching the Earth's surface.

Solar zenith angle (SZA) — The solar zenith angle is the angle between the sun's rays and the local upward vertical, measured in degrees from 0° (overhead sun) to 90° (sun at the horizon).

Spectral irradiance — The radiation at the Earth's surface measured at each wavelength of the full UV spectrum.

Squamous cell carcinoma (SCC) — Squamous cell carcinoma is the second most common form of keratinocyte cancer in humans. It begins in the cells in the outer part of the skin and is thought to be primarily caused by exposure to ultraviolet radiation. Squamous cell carcinoma may grow quickly and spread to other parts of the body, making it a dangerous form of skin cancer.

Super-recovery — A projection of stratospheric ozone levels that allows ozone to attain levels greater than the "baseline" values observed in 1979–1980. This projection assumes that the observed correlation between EESC and ozone can be extrapolated to higher-than-observed ozone levels as well as the lower levels upon which ozone depletion projections depend. It implies that ozone depletion caused by ODS was already underway before observations began.

Total Ozone Mapping Spectrometer (TOMS) — A satellite-based instrument used to measure the total vertical column of ozone in the atmosphere. The method is based on detecting UV radiation backscattered by the lower atmosphere after it passes through stratospheric ozone. The amount of ozone is determined by comparing the backscattered radiation at several pairs of wavelengths, selected for different sensitivity to absorption by ozone. The TOMS instrument aboard the Nimbus-7 satellite provided nearly continuous global ozone data from late 1978 to early 1993. Shorter data records from more recent satellites (Meteor-3, Earth Probe, Ozone Monitoring Instrument [OMI]) are also available.

Ultraviolet (UV) radiation — UV radiation is a portion of the electromagnetic spectrum with wavelengths shorter than visible light. The sun produces UV radiation, which is commonly split into three arbitrarily defined bands: UV-A, UV-B, and UV-C. Because the AHEF relies on action spectra equations to estimate health effects, it is not necessary to define the exact wavelengths that make up each band. UV-A is not absorbed by ozone. UV-B is mostly absorbed by ozone, although some reaches the Earth. UV-C is completely absorbed by ozone and normal oxygen. The AHEF uses the percentage change in exposure to UV radiation multiplied by the appropriate BAF and the age-specific baseline incidence or mortality rate to predict future changes in human health effects. Although the AHEF considers only solar UV radiation, exposure to UV radiation from artificial sources (e.g., tanning beds, welding, mercury lamps) is also associated with adverse health effects.

UV-A — A band of ultraviolet radiation with wavelengths from 320–400 nanometers produced by the sun. UV-A is not absorbed by ozone. This band of radiation has wavelengths just shorter than visible violet light.

UV-B — A band of ultraviolet radiation with wavelengths from 280–320 nanometers produced by the sun. UV-B has been associated with human health impacts and is particularly effective at damaging DNA. UV-B has been identified as a cause of melanoma and other types of skin cancer as well as cataract and suppression of the immune system. It has also been linked to damage to some materials, crops, and marine organisms. The ozone layer protects the Earth against most solar UV-B radiation.

UV-C — A band of ultraviolet radiation with wavelengths shorter than 280 nanometers. UV-C is extremely dangerous, but it is completely absorbed by ozone (at wavelengths between 240 and 280 nm) and normal oxygen (O_2) (at wavelengths between 200 and 280 nm), and hence does not reach the Earth's surface.

Appendix B. ODS Parameters

Table B.1 includes the ODS parameters used to inform the EESC and Ozone Sub-model calculations for all ODS modeled in the AHEF. The lifetimes from the WMO 2018 Assessment were used for calculations in this report. WMO 2011 values were used in the 2015 AHEF report and are listed for context.[16]

Table B.1. ODS parameters used in the AHEF

Scenarios	Lifetime (years)[a]		Stratospheric Chlorine Release Factor[b]	Alpha Factor[b]	Number of Chlorine Atoms	Conversion Factor (kt/ppt)
	WMO 2018[c]	WMO 2011[d]				
CFC-11	**52**	45	0.47	0	3	24.5
CFC-12	**102**	100	0.23	0	2	23.1
CFC-113	**93**	85	0.29	0	3	33.3
CFC-114	**189**	190	0.12	0	2	30.4
CFC-115	**540**	1020	0.04	0	1	27.5
HCFC-22	**12**	11.9	0.13	0	1	15.4
HCFC-141b	**9.4**	9.2	0.34	0	2	20.6
HCFC-142b	**18**	17.2	0.17	0	1	17.8
Halon 1301	**72**	65	0.28	60	0	26.5
Halon 1211	16	16	0.62	60	1	29.4
Halon 2402	**28**	20	0.65	120	0	46.3
Halon 1202	**2.5**	2.9	0.62	120	0	37.3
CH_3Br	0.8	0.8	0.6	60	0	16.9
CCl_4	26	26	0.56	0	4	27.4
CH_3CCl_3	5	5	0.67	0	3	23.7
CH_3Cl	**0.9**	1	0.44	0	1	9

[a]Values updated since the AHEF 2015 report are shown in bold.
[b]Stratospheric Chlorine Release and alpha factors are unchanged since the AHEF 2015 report.
[c]This report uses factors from the WMO 2018 Assessment, Table A1 (WMO 2018).
[d]The AHEF 2015 report used values from the WMO 2011 assessment (WMO 2011).

[16] The AHEF 2015 report presented values from the WMO 2014 Assessment, but they were not released in time to be included in the calculations. WMO 2018 Assessment values are unchanged from WMO 2014.

Appendix C. Discussion of Assumptions at Simulation End

As noted in Sections II.1.2 and III.5.1, the assessment of future health benefits of various ODS control strategies relative to each other, or to no controls, is extremely sensitive to assumptions made about future environmental and population conditions and to the time horizon of the calculation. This appendix details the assumptions made and presents results that illustrate the sensitivity of the calculation end stages, or "termination."

DEFINITIONS:

"**Termination**" describes the treatment of the later stages of the exposure/effects calculation. Recovery scenarios are relatively insensitive to termination details. Runaway scenarios are extremely sensitive to termination details, and this sensitivity increases with time.

"**Recovery scenarios**" are situations where ozone levels are projected to return to pre-1980 values after a period of depletion. The current Montreal Protocol as amended and adjusted ("WMO A1") yields a recovery scenario, with ozone projected to return to pre-1980 levels around the year 2045.

"**Runaway scenarios**" are situations where projected ozone depletion continues to increase into the future. Both the unregulated "No Controls" and original Montreal Protocol ("MP'87") emissions scenarios fall into this category.

"**Catastrophic conditions**" are those points in a runaway scenario beyond which we have no confidence in our calculation results. Note that, in any case, confidence in the results decreases progressively as the simulation moves further away from current conditions.

There are several different calculation inputs to the health effect projections whose termination treatment must be considered in the AHEF:

1. We hold annual EESC (and therefore monthly ozone) constant after 2100.
2. We constrain monthly ozone values to remain between an upper limit of their 1980 values and a lower limit of 100 DU, even if the greatly extrapolated (and therefore increasingly uncertain) EESC/ozone relationship suggests it should exceed those limits.
3. We hold population constant after 2060, since U.S. census projections are not currently available beyond that point. The proportions of various racial groups are also held constant after 2060. See Appendix E for a discussion of the assumptions regarding relationships between reported race and skin type-related health effect susceptibility.
4. The health effect incidence data is held constant for each age group after 1995–2000, as in the 2015 AHEF report. The 2006 AHEF report attributed historical incidence increases to changes in individual behavior. We note that health effect incidence has been observed to increase after 2000 and that the year-2000 endpoint used here is an arbitrary assumption.
5. We use one of two options for the end point of the calculation. The first option cuts off all calculations at 2100. The second option, as used in previous AHEF reports, considers natural aging beyond 2100 for cohorts already born (without allowing new births). This extends the potential timescale for the realization of calculated effects to almost 2200.

Endpoints Used in this Report to Calculate U.S. Health Effects of ODS

1. Calculation through 2100

Health effects are calculated for each year to 2100. The termination points of the various calculation inputs (e.g., population growth) minimally affect the results owing to the delayed manifestation of most health effects.

2. Extended calculation for people in birth cohorts through 2100

Health effects are calculated for the entire lifetime of people born in all birth cohorts between 1890 (encompassing years 1888–1892) and 2100 (encompassing years 2098–2102). This analysis accounts for all effects arising from 21st century exposure by extending the cumulative exposure to UV radiation calculation far into the 22nd century. The results are extremely sensitive to termination points for the various calculation inputs, as shown in the figures below.

The year or cohort year 2100 is chosen as an endpoint for calculations in this report to provide consistency with previous AHEF reports and to align with projections in the generally accepted literature on ozone depletion (e.g., WMO 2014 and 2018). Projections from the AHEF become more sensitive to initial assumptions the further in the future the endpoint is set, especially for runaway scenarios.

Figure C.1 shows annual exposure to UV radiation to 2100 in the 30°–40°N latitude band calculated for the three ODS control scenarios presented in this report, WMO A1, MP'87, and "No Controls." The two panels show the same values at different scales. The vertical dashed line in the right panel indicates the point where catastrophic conditions are reached in the "No Controls" simulation. Exposure to UV radiation is expressed as UV weighted by the SCUP-h action spectrum, in units of KJ $m^{-2}y^{-1}$. The Montreal Protocol as amended and adjusted ("WMO A1") is a recovery scenario, with exposure to UV radiation returning to baseline levels around 2045. By contrast, the "No Controls" scenario and even the original Montreal Protocol ("MP'87") are runaway scenarios. Catastrophic conditions are reached after 2065 in the "No Controls" scenario, when summertime ozone values rapidly crash toward their arbitrary lower limit of 100 DU (as evidenced by the UV radiation plateau beginning in 2080). The MP'87 simulation shows lower-limit ozone values only in winter prior to 2100, and in summer after 2100. If this simulation were continued further, it would likely assume a UV radiation profile similar to the No Controls case but delayed by ~40 years.

Figure C.1. Projected annual exposure to UV radiation for 30°–40°N

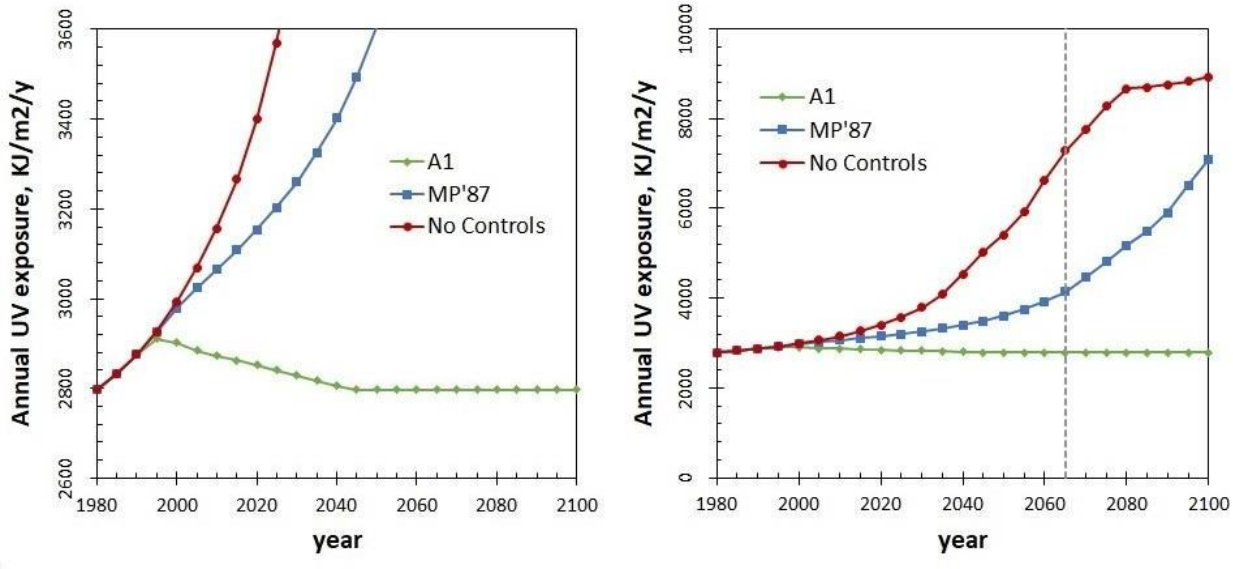

Figure C.2 shows the cumulative health effects responses for the various ODS emission scenarios, by year through 2100. By this date, cumulative response has almost stopped rising for the WMO A1 scenario, whereas it is rising ever more steeply for the runaway scenarios. It is clear that an assessment of “health benefits” (sometimes known as “cases avoided”) under the WMO A1 scenario relative to either of the other two scenarios will be very different whether the calculation is terminated at 2100 or extended to follow all birth cohorts from 1890–2100 for their entire lifespans, and into the region where projected “catastrophic conditions” are influential.

Figure C.2. U.S. cumulative incremental health effects for three ODS emission scenarios

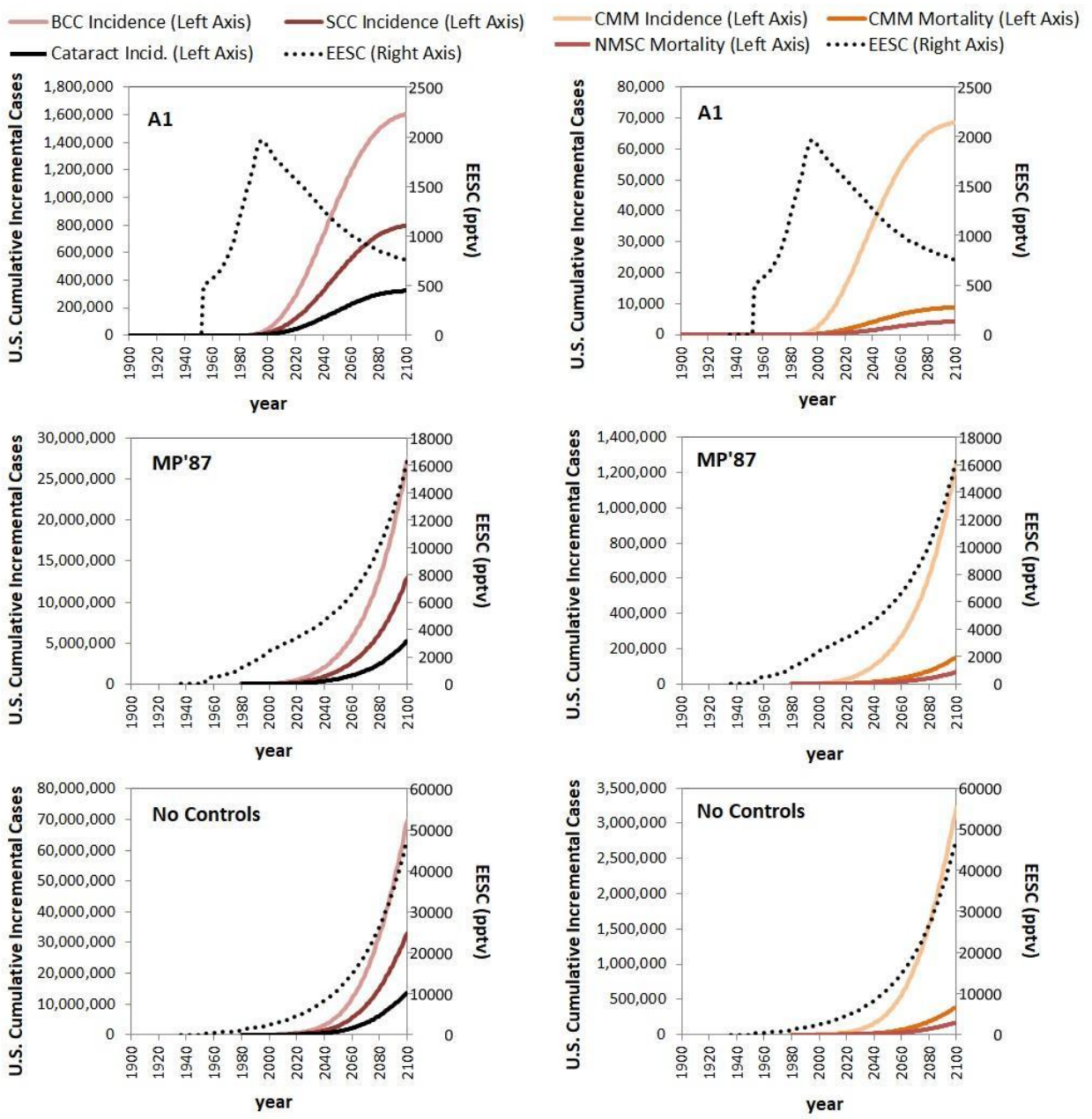

The influence of endpoint selection is illustrated in Figure C.3, for the No Control case. The MP'87 case (not depicted) yields similar patterns, with values roughly one-third of those in the No Control case. Solid lines show calculations terminating in 2100 and dashed lines show calculations extended throughout the lifetimes of all cohorts born through 2100 ±2 years. If the calculation is terminated in 2100, health effects are considered over the entire lifetimes of cohorts born in the first decade or two of the 21st century. Later cohorts survive beyond 2100, so progressively less of their lifespans is included in the analysis. However, many projected health

effects do not manifest until the 22nd century. If the calculation is extended beyond 2100 to follow all study cohorts born through 2100 for their entire lives (dashed lines), we move into the region of catastrophic conditions. Here, projected health effects increase significantly and contain significant uncertainty. Additionally, the leveling-off of the incidence and mortality curves for the later cohorts in the extended simulations result from termination points in ozone depletion and population growth.

Figure C.3. Selected health effects for the No Controls case for calculations terminating in 2100 vs. calculations extending throughout the lifetimes of all cohorts born through 2100

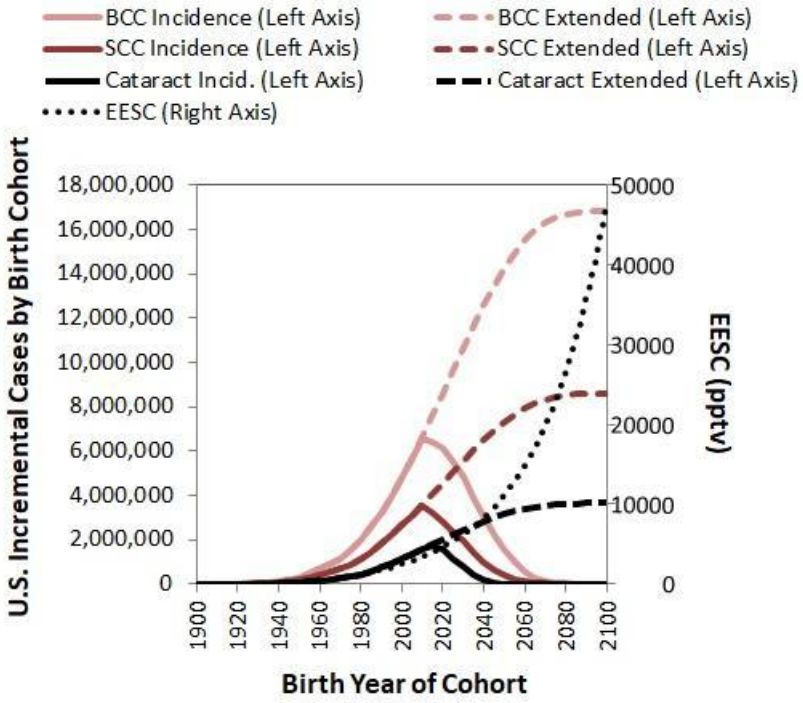

Appendix D. Effects of Early-life Exposure Weighting

Early-life exposure to UV radiation is a potentially important risk factor for melanoma,[17] with manifestation delayed for possibly decades.[18] The AHEF allows the option of using weighting factors to include only the contributions of exposure to UV exposure radiation through age 20 in the estimate of later-life health effects. Figure D.1 compares U.S. incremental melanoma mortality calculated using whole-life exposure to UV radiation and using only exposure gained during ages 1–20. Estimated U.S. melanoma mortality in the early-life exposure case peaks about 30 years after that in the whole-life exposure case and about 70 years after the minimum ozone values—the period of maximum UV exposure to UV radiation.

Figure D.1. U.S. incremental melanoma mortality under the WMO A1 ODS emissions scenario for cumulative exposure with equal age exposure weighting and with weighting of exposures for ages 1–20 only

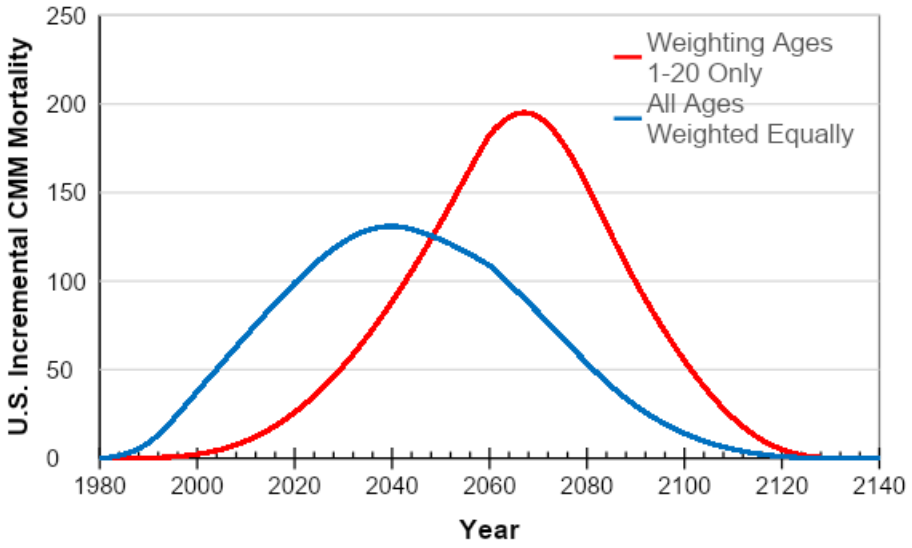

[17] Harrison et al., 1994; Zanetti et al., 1992
[18] Geller et al., 1998

Appendix E. Sensitivity of Effects Calculations to Assumptions About Race

Population data available from the U.S. Census Bureau has become more detailed in recent years, such that surveyed individuals may self-report their race in one or a combination of five different groupings. The available health effects data, on the other hand, are categorized in terms of “light-skinned” and “dark-skinned” populations. Thus, a calculation for health effects in the U.S. population must make assumptions about the relevance of the terms “light-skinned” and “dark-skinned” for the different racial groups in the population. We make the assumption that those who self-report race as “White” and no other races are light-skinned, and those who self-report as “Black or African American” and no other races to be dark-skinned. We then group those who self-report as “Asian”, “American Indian or Alaska Native”, “Native Hawaiian or Other Pacific Islander”, or any combination of races into an “Other” category.

Skin cancer incidence and mortality rates and BAFs are consistently higher in the data for light-skinned than for dark-skinned populations. It is reasonable to conjecture that the average rates of health effects in the “other” populations lie somewhere between the “light” and “dark” extremes. Thus, a range of possible health effect totals may be estimated by combining the “Other” populations alternately with the “White” and “Black” populations. These two cases are expected to represent the high- and low-end estimates, respectively, of the range of national cancer incidence and mortality totals.

As noted in Section III.5.2, the health effects calculations detailed in the main body of this report categorize the “Other” population as “light-skinned” and so represent the high end of the range of possible skin cancer estimates. This Appendix presents results for the same calculations, performed with the “Other” population instead categorized as “dark-skinned.” In general, the dark-skinned option gives lower results than the light-skinned option for skin cancer effects, depending on the scenario and time horizon. Present-day values show the smallest differences (results for the dark-skinned option are 1% to 8% lower), while long-term calculations show differences between 11% and 17%. The increase in differences with longer time horizons results from the fact that the fraction of the U.S. population included in the “Other” category increases as time goes on (the population becomes more diverse).

Cataract incidence shows a small (and probably insignificant) increase upon going from light skin to dark skin, since the BAFs for cataract are slightly lower for light-skinned than for dark-skinned populations. This small difference must be a function of behavior, since eye physiology is not related to skin pigment.

Table E.1. Recalculation of Table 1 assigning all "Other" race categories as "dark-skinned" instead of "light-skinned." The table shows annual average U.S. melanoma incidence (2007–2011) and mortality (2006–2010) and keratinocyte incidence (2006–2010) calculated with the AHEF, compared with observational and modeled data.

Health Effect	Data Source	Male	Female	Total
Melanoma Incidence 2007–2011	AHEF	33,000	32,000	65,000
	U.S. DHHS (observed)	37,000	27,000	63,000
	IHME (modeled)	41,000	30,000	71,000
Melanoma Mortality 2006–2010	AHEF	4,600	3,100	7,800
	U.S. DHHS	5,700	3,000	8,800
	IHME	5,700	3,200	8,900
Squamous Cell Carcinoma Mortality 2006–2010	AHEF	1,700	900	2,600
	IHME	2,100	900	3,000

Note: Totals may not sum due to independent rounding.

Table E.2. Recalculation of Table 2 assigning all "Other" race categories as "dark-skinned" instead of "light-skinned." The table shows calculated incremental U.S. health benefits of the Montreal Protocol as amended and adjusted (emissions scenario WMO A1) relative to no controls and to the original (1987) Montreal Protocol through the lifetimes of people born 1890–2100.

		Health effects avoided by Montreal Protocol as amended and adjusted, compared to no ODS controls	Additional health effects avoided by Montreal Protocol with amendments and adjustments relative to 1987 Montreal Protocol
Skin Cancer Incidence	Keratinocyte	367,000,000	196,000,000
	Melanoma	9,600,000	5,100,000
	Total	377,000,000	201,000,000
Skin Cancer Mortality	Keratinocyte	700,000	400,000
	Melanoma	1,300,000	700,000
	Total	2,000,000	1,100,000
Cataract Incidence		66,000,000	35,000,000

Note: Totals may not sum due to independent rounding.

Table E.3. Recalculation of Table 3 assigning all "Other" race categories as "dark-skinned" instead of "light-skinned." The table shows calculated incremental U.S. health benefits of the Montreal Protocol as amended and adjusted (WMO A1) relative to no controls and to the original (1987) Montreal Protocol for years 1980–2100.

		Health effects avoided by Montreal Protocol as amended and adjusted relative to no ODS controls	Additional health effects avoided by Montreal Protocol as amended and adjusted relative to 1987 Montreal Protocol
Skin Cancer Incidence	Keratinocyte	85,000,000	32,000,000
	Melanoma	2,000,000	1,000,000
	Total	88,000,000	33,000,000
Skin Cancer Mortality	Keratinocyte	140,000	60,000
	Melanoma	320,000	120,000
	Total	470,000	180,000
Cataract Incidence		14,000,000	5,000,000

Note: Totals may not sum due to independent rounding.

Table E.4. Recalculation of Table F.1. assigning all "Other" race categories as "dark-skinned" instead of "light-skinned." The table shows calculated U.S. health impacts of unexpected emissions of CFC-11 compared with the Montreal Protocol as amended and adjusted (WMO A1) standard scenario for years 2011–2050.

Scenarios	Skin Cancer Mortality			Skin Cancer Incidence			Cataract Incidence
	Keratinocyte	Melanoma	Total	Keratinocyte	Melanoma	Total	
Extended Scenario	35	80	120	21,700	700	22,500	3,200
2025 Scenario	20	50	70	12,400	400	12,800	1,800
2020 Scenario	10	30	40	7,200	200	7,400	1,300
Bank Scenario	20	40	60	11,600	400	11,900	1,700

Note: Totals may not sum due to independent rounding.

Table E.5. Recalculation of Table F.2. assigning all "Other" race categories as "dark-skinned" instead of "light-skinned." The table shows calculated U.S. health effects of unexpected emissions of CFC-11 compared with the Montreal Protocol as amended and adjusted (WMO A1) standard scenario for years 2011–2100.

Scenarios	Skin Cancer Mortality			Skin Cancer Incidence			Cataract Incidence
	Keratinocyte	Melanoma	Total	Keratinocyte	Melanoma	Total	
Extended Scenario	190	400	600	111,400	3,200	114,600	18,200
2025 Scenario	80	160	240	44,800	1,300	46,000	7,400
2020 Scenario	40	90	130	24,000	700	24,700	4,000
Bank Scenario	80	160	240	45,400	1,300	46,700	7,500

Note: Totals may not sum due to independent rounding.

Table E.6. Recalculation of Table F.3. assigning all "Other" race categories as "dark-skinned" instead of "light-skinned." The table shows calculated U.S. health effects of unexpected emissions of CFC-11 compared with the Montreal Protocol as amended and adjusted (WMO A1) standard scenario for population cohorts born 1890–2100.

Scenarios	Skin Cancer Mortality			Skin Cancer Incidence			Cataract Incidence
	Keratinocyte	Melanoma	Total	Keratinocyte	Melanoma	Total	
Extended Scenario	250	480	720	133,100	3,600	136,700	21,800
2025 Scenario	90	180	270	50,200	1,400	51,600	8,100
2020 Scenario	50	100	140	26,500	700	27,200	4,300
Bank Scenario	100	180	280	51,700	1,400	53,100	8,500

Note: Totals may not sum due to independent rounding.

Appendix F. Estimation of Incremental Health Effects of Additional CFC-11 Emissions

Recent measurements of atmospheric concentrations suggest that concentrations of CFC-11 have decreased at a rate slower than expected under full implementation of the Montreal Protocol as amended and adjusted (Montzka et al., 2018; Rigby et al., 2019). The AHEF model can be used to examine deviations from the expected phaseout of certain ODS, including the effects on global EESC, seasonal and latitudinal changes in stratospheric ozone and ground-level UV radiation, and estimates of associated disease (i.e., melanoma and keratinocyte cancer, and cataract).

To estimate the potential health effects of unexpected CFC-11 emissions, four scenarios were developed and run in the AHEF, as described in the box below. In the first three scenarios, emissions for the years 2011–2013 were estimated as 63.5 Gg/yr by averaging two estimates of historical CFC-11 emissions (Montzka et al., 2018; Rigby et al., 2019). In 2014, CFC-11 emissions were estimated to increase to 77.5 Gg/yr. In the fourth scenario, CFC-11 emissions were estimated based on Dhomse et al. (2019), which constructs an emissions scenario curve based on initial rapid increase in CFC-11 emissions and slower release from accumulated CFC-11 banks. This scenario first takes the estimate of 13 Gg/year in new emissions due to unreported production and assumes an immediate production release rate of 15 percent followed by 3.5 percent/year. This creates a gradually decreasing emissions curve where CFC-11 emissions continue past 2100 due to releases from the accumulated bank even after production goes to zero.

Each scenario makes a different assumption about the length of time the increased emissions continue, as shown in the box and Figure F.1 below. The additional emissions were applied to the WMO A1 CFC-11 emissions profile.

Scenarios for Increased Emissions of CFC-11

Extended Scenario – CFC-11 emissions continue at 77.5 Gg/yr from 2014 indefinitely.

2025 Scenario – CFC-11 emissions continue at 77.5 Gg/yr from 2014–2024 and revert to those expected under the WMO A1 scenario in 2025.

2020 Scenario – CFC-11 emissions continue at 77.5 Gg/yr from 2014–2019 and revert to those expected under the WMO A1 scenario in 2020.

Bank scenario – CFC-11 emissions begin increasing in 2012 above those expected under the WMO A1 scenario, peaking around 77 Gg/yr in 2015–2017, then declining sharply through 2100.

Figure F.1 WMO A1, Extended Scenario, 2025 Scenario, 2020 Scenario, and Bank Scenario CFC-11 emissions

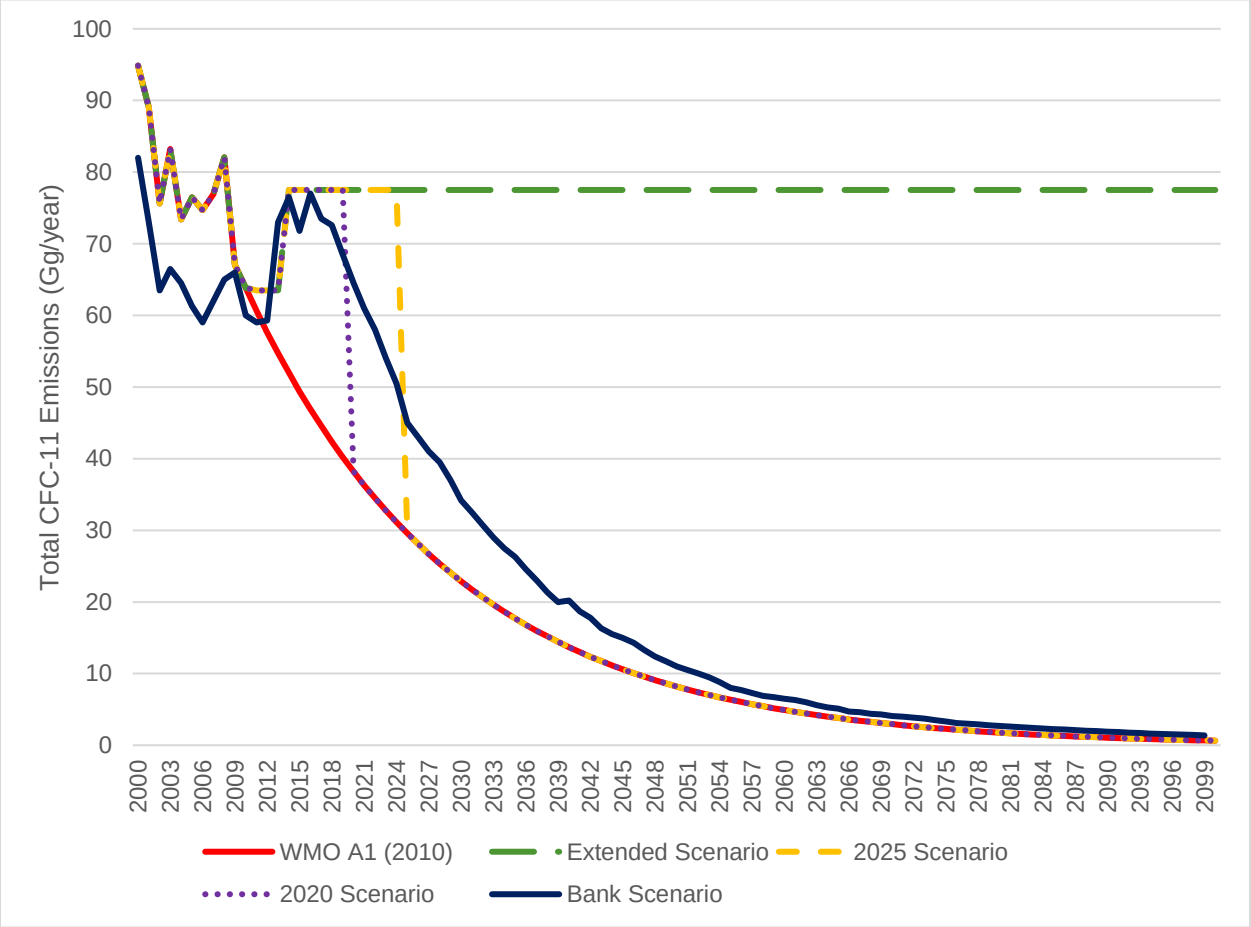

Among the four scenarios, the Extended Scenario and the Bank scenario most closely align with the 2018 Scientific Assessment of Ozone Depletion report, which found that "[i]f total emissions of CFC-11 were to continue at levels experienced from 2002–2016 (67 Gg/yr), the return of mid-latitude […] EESC to the 1980 value would be delayed by about seven years" (WMO, 2018). The AHEF models an approximately eight-year delay in ozone recovery associated with the Extended Scenario.

Tables F.1, F.2, and F.3 show the health impacts from 2011–2050, 2011–2100, and for the entire lifetimes of birth cohorts through 2100 respectively.[19]

[19] One key influence in this calculation is that the standard AHEF model specifies that once EESC drops below 1980 levels (~1200 pptv), ozone recovery is complete—i.e., ozone is maintained at the 1980 values if EESC < 1200 pptv. This point is reached in 2045 under the WMO A1 emissions scenario. Accordingly, small changes in EESC after this date have no effect on the standard calculation, since the net EESC continues to decrease while ozone levels remain constant. This means that additional emissions, even those with long-term effects on EESC, do not affect exposure to UV radiation after the ozone recovery point specified in the calculation. This situation is a direct consequence of the choice of 1980 as the year that defines full recovery.

Table F.1. U.S. health impacts of unexpected emissions of CFC-11 compared with the Montreal Protocol as amended and adjusted (WMO A1) standard scenario for years 2011–2050

Scenarios	Skin Cancer Mortality			Skin Cancer Incidence			Cataract Incidence
	KC	Melanoma	Total	KC	Melanoma	Total	
Extended Scenario	40	100	140	24,800	800	25,700	3,100
2025 Scenario	20	60	80	14,100	500	14,600	1,800
2020 Scenario	10	30	40	8,100	300	8,400	1,000
Bank Scenario	20	50	70	13,200	450	13,600	1,600

Note: Mortality figures have been rounded to the nearest ten and incidence figures to the nearest hundred. Totals may not sum due to independent rounding.

The continued emissions of CFC-11 are estimated to result in fewer avoided cancers and cataract cases. The Extended Scenario emissions are estimated to result in a loss of an avoided 24,800 cases of keratinocyte cancer and 800 cases of melanoma, for a total of 25,700 cancer cases, through the year 2050, as seen in Table F.1. The Extended Scenario is also estimated to result in the loss of 40 avoided deaths from keratinocyte cancer and 100 from melanoma, totaling 140 avoided deaths forgone in the United States, as well as 3,100 cataract cases. Scenarios with shorter periods of additional CFC-11 emissions are expected to result in fewer lost health benefits.

The 2025 Scenario is estimated to forgo 14,100 keratinocyte cancers and 500 melanomas, for a total of 14,600 cases of cancer that would have been avoided without the additional emissions. The 2025 Scenario is also estimated to lose 80 avoided skin cancer deaths—20 from keratinocyte cancer and 60 from melanoma—and 1,800 cataract cases through 2050. Similarly, the Bank Scenario is estimated to result in the loss of 13,200 keratinocyte cancers and 450 melanomas avoided, for a total of 13,600 cases of skin cancer. The Bank Scenario is also estimated to forgo 70 skin cancer deaths—20 from keratinocyte cancer and 50 from melanoma—and 1,600 cataract cases avoided through 2050.

The 2020 Scenario is estimated to result in 8,100 cases of keratinocyte cancer and 300 cases of melanoma, for a total of 8,400 additional skin cancers over the same time period. It is also expected to cause 10 deaths from keratinocyte cancer and 30 from melanoma, for a total of 40 additional deaths. This scenario is also expected to result in 1,000 additional cataract cases in the United States through 2050.

Table F.2. U.S. health effects of unexpected emissions of CFC-11 compared with the Montreal Protocol as amended and adjusted (WMO A1) standard scenario for years 2011–2100

Scenarios	Skin Cancer Mortality			Skin Cancer Incidence			Cataract Incidence
	KC	Melanoma	Total	KC	Melanoma	Total	
Extended Scenario	220	480	700	130,700	3,800	134,500	17,400
2025 Scenario	90	190	280	52,300	1,500	53,800	7,100
2020 Scenario	50	100	150	27,900	800	28,700	3,800
Bank Scenario	90	190	280	53,000	1,500	54,500	7,100

Note: Mortality figures have been rounded to the nearest ten and incidence figures to the nearest hundred. Totals may not sum due to independent rounding.

The estimated health effects in Table F.2 result from the same CFC-11 emission scenarios and are accumulated through 2100 instead of 2050. The Extended Scenario emissions are expected to forgo 130,700 keratinocyte cancer cases and 3,800 cases of melanoma, totaling 134,500 cases of skin cancer, that would have been avoided without those emissions. This scenario is estimated to lose an avoided 220 deaths due to keratinocyte cancer and 480 from melanoma, for a total of 700 additional deaths through 2100. This scenario is expected to forgo 17,400 cases of cataract avoided as well.

The 2025 Scenario results in an estimated 52,300 cases of keratinocyte cancer and 1,500 cases of melanoma, for a total of 53,800 fewer avoided cancers. These cancers are calculated to lead to an additional 90 deaths from keratinocyte cancer and 190 from melanoma, totaling a loss of 280 cancer deaths avoided through 2100. The 2025 Scenario is estimated to lose an avoided 7,100 cataract cases in that timeframe. Similarly, the Bank Scenario results in an estimated 53,000 cases of keratinocyte cancer and 1,500 cases of melanoma, for a total of 54,500 fewer avoided cancers. These cancers are calculated to lead to an additional 90 deaths from keratinocyte cancer and 190 from melanoma, totaling a loss of 280 cancer deaths avoided through 2100. The Bank Scenario is estimated to forgo 7,100 cataract cases avoided in that timeframe.

For CFC-11 emissions stopping in 2020, an estimated loss of an avoided 27,900 cases of keratinocyte cancer and 800 cases of melanoma will occur in the United States, totaling 28,700 skin cancer cases. These cancers are calculated to lead to an additional 50 deaths from keratinocyte cancer and 100 from melanoma, totaling a loss of 150 cancer deaths avoided through 2100. The 2020 scenario is estimated to forgo 3,800 cataract cases avoided in that timeframe.

The estimated health effects in Table F.3 result from the same CFC-11 emission scenarios for cohorts born in years 1890 through 2100, to align with the usual presentation of results. The Extended Scenario is expected to see 155,200 fewer keratinocyte cancer cases and 4,400 fewer cases of melanoma avoided, totaling a loss of 159,600 cases of skin cancer avoided. This scenario is estimated to forgo the prevention of 280 deaths due to keratinocyte cancer and 560 from melanoma, forgoing a total of 840 deaths avoided through 2100. This scenario is expected to result in 121,200 fewer cataract cases avoided as well.

Table F.3. U.S. health effects of unexpected emissions of CFC-11 compared with the Montreal Protocol as amended and adjusted (WMO A1) standard scenario for population cohorts born in years 1890–2100

Scenarios	Skin Cancer Mortality			Skin Cancer Incidence			Cataract Incidence
	KC	Melanoma	Total	KC	Melanoma	Total	
Extended Scenario	280	560	840	155,200	4,400	159,600	121,200
2025 Scenario	100	220	320	58,200	1,700	59,800	7,800
2020 Scenario	50	110	170	30,700	900	31,600	4,100
Bank Scenario	120	220	340	57,900	1,700	59,600	9,300

Note: Mortality figures have been rounded to the nearest ten and incidence figures to the nearest hundred. Totals may not sum due to independent rounding.

The 2025 Scenario emissions lead to an estimated 58,200 cases of keratinocyte cancer and 1,700 cases of melanoma that would have been avoided without those emissions, for a total loss of 59,800 cancers avoided. These cancers are calculated to lead to an additional 100 deaths from keratinocyte cancer and 220 from melanoma, totaling a loss of 320 avoided cancer deaths through 2100. The 2025 Scenario is estimated to lose an avoided 7,800 cataract cases in that timeframe. Similarly, the Bank Scenario forgoes prevention of an estimated 57,900 cases of keratinocyte cancer and 1,700 cases of melanoma, for a total of 59,600 cancers. These cancers are calculated to lead to an additional 120 deaths from keratinocyte cancer and 220 from melanoma, totaling 340 avoided cancer deaths lost through 2100. The 2025 Scenario is estimated to forgo 9,300 avoided cataract cases in that timeframe.

For CFC-11 emissions stopping in 2020, fewer health benefits from reduced ODS emissions will be lost than in the other scenarios. An estimated 30,700 fewer cases of keratinocyte cancer and 900 fewer cases of melanoma will be avoided in the United States, totaling 31,600 skin cancer cases. These cancers are calculated to lead to an additional 50 deaths from keratinocyte cancer and 110 from melanoma, totaling a loss of 170 cancer deaths avoided through 2100. The 2020 Scenario is estimated to forgo 4,100 cataract cases avoided in that timeframe.

Comparing the estimates in the three tables highlights the importance of modeling a sufficiently long time period after ODS emissions to capture the resulting health effects that occur decades later. For example, in the 2020 Scenario, the last emissions of “additional” CFC-11 occurs in 2019. In Table F.1, looking at excess health effects occurring through 2050, we see that the CFC-11 emissions are estimated to lead to 8,400 cases avoided and 40 deaths from skin cancer avoided. Compare this with the results in Table F.2 for the same scenario but now capturing health effects from 2051–2100 as well. Now the same emissions are estimated to forgo an avoided 28,700 cases of cancer and 150 deaths. Even though the emissions stopped more than 30 years prior to the 2050 cutoff for Table F.1, the long lifetime of CFC-11 in the atmosphere and the potentially long delay in manifestation of disease after exposure means that more than twice as many health benefits are lost from 2051–2100 as from 2011–2050. Extending the window even further as in Table F.3 increases the estimated health effects further, but not nearly as much as the difference between Table F.1 and Table F.2, with an estimated 31,600 fewer total cases of skin cancer avoided and 170 fewer deaths avoided. This shows that most health effects from CFC-11 emissions in the early part of this century will accrue before 2100.